Contribution from the Research School of Chemistry, The Australian National University, Canberra, Australia 2600, and the Department of Chemistry, University of Otago, Dunedin, New Zealand

Absence of Common Intermediates in the Induced Reactions of Cobalt(III) Complexes. Hg^{2+}- and NO^+-Induced Aquation and Base Hydrolysis of $[Co(Me(tren))(NH_3)X]^{3+/2+}$ Species: Crystal and Strain-Energy-Minimized Structures of the *s* and *p* Isomers of the $[Co(Me(tren))(NH_3)Cl]^{2+}$ Ion

DAVID A. BUCKINGHAM,* JULIAN D. EDWARDS, and GEORGE M. McLAUGHLIN

Received July 6, 1981

The synthesis of 2-(methylamino)-2′,2″-diaminotriethylamine (Me(tren)) is described as are the preparations of $[Co(Me(tren))(NO_2)_2]Cl$, $[Co(Me(tren))Cl_2]Cl$, *t*-, *anti-p*-, *syn-p*-, and *s*-$[Co(Me(tren))(NH_3)Cl]^{2+}$ salts, and *anti-p*-, *syn-p*-, and *s*-$[Co(Me(tren))(NH_3)X](ClO_4)_2$ (X = Br, N_3); the resolutions of *t*- and *anti-p*-$[Co(Me(tren))(NH_3)Cl]Cl_2$ are described. The anti-*p*, syn-*p*, and *s* isomers are characterized by crystal structures on *anti-p*-(*RS*)-$[Co(Me(tren))(NH_3)Cl](ZnCl_4)$ ($P2_1/c$, $Z = 4$, 1989 unique reflections ($>3\sigma(I)$), $R = 0.038$), *anti-p*-(*S*)-$[Co(Me(tren))(NH_3)Cl](ZnCl_4)$ ($P2_12_12_1$, $Z = 4$, 2292 unique reflections ($>3\sigma(I)$), $R = 0.038$), and *s*-(*RS*)-$[Co(Me(tren))(NH_3)Cl](ZnCl_4)\cdot H_2O$ ($P2_1/n$, $Z = 4$, 1424 unique reflections ($>3\sigma(I)$), $R = 0.053$). The rates of aquation (k_{aq}), Hg^{2+}-induced aquation (k_{Hg}), and base hydrolysis (k_{OH}) are reported for the different $[Co(Me(tren))(NH_3)Cl]^{2+}$ isomers with the different orders syn-*p* > *s* > anti-*p* for k_{aq} and k_{Hg} (2.95 (0.1) × 10^{-5} s^{-1} and 1.84 (0.04) mol^{-1} dm^3 s^{-1}, 1.1 (0.1) × 10^{-5} s^{-1} and 0.34 (0.03) mol^{-1} dm^3 s^{-1}, 1.95 (0.05) × 10^{-6} s^{-1} and 2.2 (0.2) × 10^{-2} mol^{-1} dm^3 s^{-1}, respectively) and anti-*p* > *s* > syn-*p* > *t* for k_{OH} (5.2 (0.2) × 10^4, 0.45 (0.02) × 10^4, 0.19 (0.02) × 10^4, and 13 mol^{-1} dm^3 s^{-1}, respectively) probably reflecting differences in N–H acidity in k_{OH}. The different rates of aquation are also reflected in the isomer distributions at equilibrium, syn-*p*:anti-*p* = 0.13 ($\Delta H°$ = 1.9 (0.2) kcal mol^{-1}) and *s*:anti-*p* = 0.35 ($\Delta H°$ = 0.7 (0.2) kcal mol^{-1}) at 25 °C, and the same relative order holds for X = OH, OH_2, and Cl. These effects probably reflect steric differences in the methyl substituent. Computer-derived structures of minimum energy closely resemble the observed crystal structures, but the final strain energies give a stability order *s* > syn-*p* > anti-*p*, which differs from experiment; however, $\Delta(\Delta U)$ is only 0.65 kcal mol^{-1} (X = Cl). The Hg^{2+}-, Ag^+-, NO^+-, and OH^--induced reactions on the pure isomers (X = Cl, Br, NH_3, N_3) give largely retention, but the precise product distributions demonstrate reagent and leaving-group sensitivity, thereby eliminating common intermediates.

Introduction

We and our colleagues continue to probe for evidence that might suggest discrete intermediates of reduced coordination number in the substitution chemistry of cobalt(III) complexes.[1-6] As the range of leaving groups extends and as the experimental precision improves, predicted lifetimes for such intermediates become shorter. The general consensus now appears to be that such species, if they exist at all, do so for at the most a few collisions within the solvent cage (i.e., $\sim 10^{-11}$ s at room temperature). We report here in detail[7] some experiments that seem to reduce this lifetime even further. These experiments were devised in an attempt to force the formation of common 5-coordinate species from a set of closely related, but chemically distinct, reactants.

It is well-known that the tetradentate ligand "tren" (2,2′,2″-triaminotriethylamine) prefers the symmetrical trigonal-bipyramidal geometry in its complexes, and this is clearly evident with M(II) ions.[8]

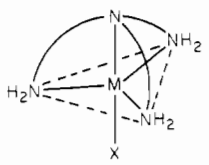

Also the substitution chemistry of the Co(III) complexes, *p*- and *t*-$[Co(tren)(NH_3)X]^{3+/2+}$ (X = NH_3, Me_2SO, NO_3^-, $MeSO_3^-$, N_3^-, Cl^-), suggests that there is a driving force toward this configuration during replacement of the X ligand.[4,9] Theory does not preclude the possibility of a trigonal-bipyramidal geometry for Co(III) and indeed suggests that a spin change could be involved if it were formed.[10] To us it appears that the tren ligand is almost the ideal in stabilizing such a geometry.

We anticipated that by using the monosubstituted *N*-methyl tren ligand (Me(tren)) in the three closely related *syn-p*-, *anti-p*-, and *s*-$[Co(Me(tren))(NH_3)X]^{3+/2+}$ isomers (Scheme I) not only would we be able to distinguish the different octahedral faces of such an intermediate but also we would be able to determine whether or not a common species of this general configuration were formed. Only ~30° bond rotations about the metal are involved, and provided this is energetically favorable, and provided the solvation sheath can adjust rapidly enough, stabilization greater than *kT* should result in a common set of products.

Included in this paper are several more general aspects of the chemistry of the $[Co(Me(tren))XY]^{3+/2+/+}$ complexes.

Experimental Section

Synthesis of 2-(Methylamino)-2′,2″-diaminotriethylamine (Me(tren)). (a) (Phenylsulfonyl)aziridine. This compound was prepared

* To whom correspondence should be addressed at the University of Otago.

(1) C. J. Boreham, D. A. Buckingham, and C. R. Clark, *Inorg. Chem.*, **18**, 1990 (1979).
(2) D. A. Buckingham, C. R. Clark, and W. S. Webley, *J. Chem. Soc., Dalton Trans.*, 2255 (1980).
(3) D. A. Buckingham, C. R. Clark, and T. W. Lewis, *Inorg. Chem.*, **18**, 2041 (1979).
(4) D. A. Buckingham, C. R. Clark, and W. S. Webley, *Aust. J. Chem.*, **33**, 263 (1980).
(5) W. G. Jackson, G. A. Lawrence, and A. M. Sargeson, *Inorg. Chem.*, **19**, 1001 (1980).
(6) D. A. Buckingham, C. R. Clark, and T. W. Lewis, *Inorg. Chem.*, **18**, 1985 (1979).
(7) The uncorrected stereochemical results of this paper were reported in summarized from previously: D. A. Buckingham, J. D. Edwards, T. W. Lewis, and G. M. McLaughlin, *J. Chem. Soc., Chem. Commun.*, 892 (1978).
(8) Approximately C_{3v} symmetry has been shown for several Cu(II), Ni(II), Zn(II), and Co(II) complexes: P. C. Jain and E. C. Lingafelter, *J. Am. Chem. Soc.*, **89**, 724 (1967); M. di Vaira and P. L. Orioli, *Acta Crystallogr.*, **B24**, 595 (1968); M. Di Vaira and P. L. Orioli, *Inorg. Chem.*, **6**, 490 (1967).
(9) D. A. Buckingham, P. J. Cresswell, and A. M. Sargeson, *Inorg. Chem.*, **14**, 1485 (1975).
(10) F. Basolo and R. G. Pearson in "Mechanisms of Inorganic Reactions", 2nd ed., Wiley, New York, 1968, p 69. The strong-field case for the d^6 ion predicts two unpaired spins for the trigonal bipyramid but none for the square pyramid.

0020-1669/82/1321-2770$01.25/0

Scheme I

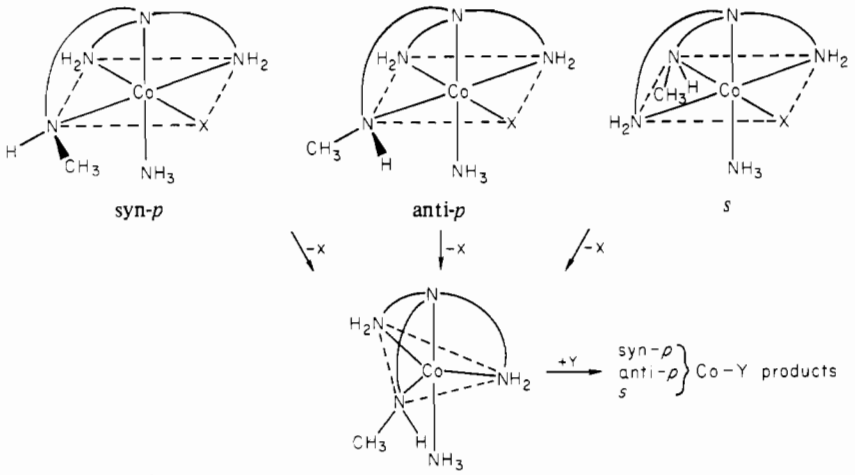

by a method based on that of Walser.[11] An aqueous 2 mol dm^{-3} NaOH solution (1 dm^3) containing ethylenimine (89 g, 2.07 mol) was cooled to −2 °C in an ice–salt–acetone bath, and benzenesulfonyl chloride (352 g, 2 mol) was added slowly with stirring over 2 h, with the temperature maintained below 0 °C to prevent polymerization. The product either immediately precipitated as white grains or was isolated from the emulsion following continued agitation of the cold solution for a further 30 min. The solid was filtered, washed with large amounts of ice-cold water and petroleum spirit, and dried over P_2O_5: yield > 90%; mp 45–46 °C (lit. mp 47–49 °C); TLC on Kieselgel 60F 254 in CH_2Cl_2–EtOAc (4:1) R_f 0.7. This material was used in the subsequent step without further purification.

(b) 2,2′-Diphthalimidodiethylamine. Phthalic anhydride (370 g, 2.5 mol) was dissolved with heating in chloroform (ca. 2 dm^3) and filtered while hot through Hyflo Supercel to remove undissolved phthalic acid. The clear solution was transferred to a large evaporating basin and cooled to 30 °C. Diethylenetriamine (102 g, 1.0 mol) dissolved in chloroform (500 cm^3) was added slowly with stirring. The reaction is slightly exothermic, and a white precipitate appeared. Chloroform was removed by heating on a steam bath and the yellow resinous mass heated in an oven for 3 h at 120 °C. After it cooled, the solid was ground in a mortar to a fine powder (this operation should be carried out in a fume hood); crude yield 400 g. The powder was washed in turn by the following solvents: water (4 dm^3, with stirring for 1 h), 4 dm^3 of 0.5 mol dm^{-3} Na_2CO_3, 4 dm^3 of ice-cold ethanol, and last water and alcohol until the washings were colorless. The residue was dried in a desiccator over concentrated H_2SO_4 and recrystallized from hot chloroform (1.5 dm^3) by addition of cold ethanol and cooling in ice. The white product was filtered and dried in vacuo. Further product was obtained by concentrating the mother liquor and cooling: yield 60%; mp 183 °C; TLC on Kieselgel 60F 254 in CH_2Cl_2–EtOAc (4:1) R_f 0.08.

(c) 2,2′-Diphthalimido-2″-benzenesulfonamidotriethylamine. Diphthalimidodiethylamine (72.6 g, 0.2 mol) was suspended in dry acetonitrile (1.2 dm^3, molecular-sieve-dried) and the mixture heated under reflux (drying tube) with mechanical stirring. A solution of (phenylsulfonyl)aziridine (55 g, 0.3 mol) in dry acetonitrile (200 cm^3) was then added over 30 min with stirring and heating. The reaction mixture slowly changed to a clear brown solution, and stirring under reflux was continued for at least 16 h. Progress was monitored by TLC (UV light) on Kieselgel 60F 254 (Merck aluminum precoated sheets) in CH_2Cl_2–EtOAc (4:1), with detection of the species diphthalimidodiethylamine (R_f 0.08), product (0.5), unknown byproduct (0.6), and (phenylsulfonyl)aziridine (0.7). When the reaction was complete, the hot solution was filtered through Hyflo Supercel and then cooled on ice, whence white crystals formed. These were removed, washed with cold acetonitrile, and dried over concentrated H_2SO_4. Further product was obtained by reducing the volume to 100 cm^3 by evaporation in vacuo: total yield 90%; mp 148 °C. Attempts to increase this scale of preparation resulted in poorer yields. Anal. Calcd for $C_{28}H_{26}N_4SO_6$: C, 61.52; H, 4.79; N, 10.25; S, 5.86. Found: C, 61.94; H, 5.03; N, 10.15; S, 5.68. ^1H NMR: δ 7.7, multiplet (13 H); 5.6, triplet (1 H); 3.7–2.6, multiplet (12 H).

(d) 2,2′-Diphthalimido-2″-(*N*-methylbenzenesulfonamido)triethylamine. 2,2′-Diphthalimido-2″-benzenesulfonamidotriethylamine (35 g, 0.064 mol) was dissolved in dry, distilled DMF (300 cm^3) contained in a 350 cm^3 Erlenmeyer flask provided with a stopper and magnetic stirrer. Oven-dried (120 °C) K_2CO_3 (35.2 g, 0.256 mol) was added, and the contents of the flask were stirred for 30 min. Freshly distilled CH_3I (5.4 cm^3, 1.4 equiv) was then added, the flask was covered with Al foil, and the contents were stirred at room temperature for 16 h. The reaction was monitored by TLC. For this an aliquot was quenched on ice and filtered and the insoluble material was washed with water and air-dried. This was dissolved in chloroform, spotted on Kieselgel 60F 254 plates, and eluted with CH_2Cl_2–EtOAc (4:1). R_f values (UV light) were as follows: starting material, 0.5; product, 0.65. Stirring was continued for 1–10 days. If at this time the reaction was not complete, more CH_3I (0.5 cm^3) was added and stirring continued (2 days). The mixture was then quenched in iced water (4 dm^3), and the yellowish solid product was removed on a filter, washed with water, and dried over concentrated H_2SO_4 (mp 171–177 °C). It was purified by dissolving in hot chloroform (200 cm^3), filtering through Hyflo Supercel, and adding acetone to induce crystallization. When the solution cooled in ice, small creamy yellow crystalline plates appeared. These were filtered and dried: yield 85%; mp 177–178 °C. Attempts to increase the scale of preparation resulted in lower yields. Anal. Calcd for $C_{29}H_{28}N_4SO_6$: C, 62.13; H, 5.03; N, 10.00; S, 5.72. Found: C, 62.44; H, 5.01; N, 9.93; S, 5.54. ^1H NMR: δ 8.0 (13 H); 4.0, 3.2 (15 H).

Some 20 g of 2,2′-diphthalimido-2″-(*N*-(^{13}C)methylbenzenesulfonamido)triethylamine was prepared by this method with (^{13}C)methyl iodide (isotopic abundance 9.6%).

(e) 2-(Methylamino)-2′,2″-diaminotriethylamine (Me(tren)). 2,2′-Diphthalimido-2″-(*N*-methylbenzenesulfonamido)triethylamine (30 g, 0.05 mol) was heated under reflux with stirring in concentrated HCl (1.2 dm^3) for 20 h. The clear colorless solution was cooled in ice and filtered to remove phthalic acid. The filtrate was evaporated to dryness and then treated with ethanol (60 cm^3) and reevaporated (twice) to remove HCl and water. The white, or clear yellow, glassy residue was dissolved in absolute ethanol (50 cm^3) with the addition of liquid NH_3 (100 cm^3). More liquid NH_3 (500 cm^3) was added followed by sodium metal (15 g) over 4 h with continuous stirring (until the mixture turned blue). The ammonia was then removed by evaporation and water (50 cm^3) added to destroy the sodium amide. This mixture was evaporated in vacuo with slight warming (<40 °C) and water (100 cm^3) added, followed by solid KOH (100 g). The amine was then extracted into ether (6 × 100 cm^3); more ether and KOH was required for complete extraction if initial addition of KOH required in an emulsion. The combined extracts were dried over Na_2CO_3 and then evaporated to yield a yellow oil. This was distilled in vacuo with use of a N_2 gas bleed, giving a clear, colorless liquid: yield 80%; bp 78–85 °C (0.2 mmHg); n^{20}_D = 1.4864. Anal. Calcd for $C_7H_{20}N_4$: C, 52.46; H, 12.58; N, 34.96. Found: C, 52.38; H, 12.47; N, 34.99. The ^1H NMR spectrum is shown in Figure 1.

A sample of (^{13}C)Me(tren) (9.6% enrichment) was prepared from 2,2′-diphthalimido-2″-(*N*-(^{13}C)methylbenzenesulfonamido)triethylamine in the same way.

(11) R. P. Walser, Dissertation, ETH Zurich, No. 4114.

Me(tren)·3HCl was obtained from anhydrous methanol by bubbling in HCl gas. It was recrystallized from methanol and dried in air. Anal. Calcd for $C_7H_{23}N_4Cl_3$: C, 31.17; H, 8.60; N, 20.78; Cl, 39.44. Found: C, 31.47; H, 8.91; N, 20.48; Cl, 39.29.

[Co(Me(tren))$(NO_2)_2$]Cl. Me(tren) (15 g, 0.094 mol) was mixed with ice-cold water (20 cm^3) and concentrated HCl (8.3 cm^3, 0.09 mol) slowly added. The ice-cold solution was added to a solution of $CoCl_2·6H_2O$ (22.3 g, 0.094 mol) in ice-cold water (30 cm^3) and $NaNO_2$ (12.9 g, 0.188 mol) immediately added followed by a vigorous stream of air at room temperature for 18 h. This yielded yellow crystals under a dark brown mother liquid. The solid product was filtered and recrystallized from hot water (yield 10 g). Anal. Calcd for $[CoC_7H_{20}N_4(NO_2)_2]Cl$: Co, 17.01; C, 24.24; H, 5.82; N, 24.24; Cl, 10.23. Found: Co, 16.68; C, 24.22; H, 5.91; N, 23.92; Cl, 10.33. The brown mother liquid was retained for subsequent use. A sample of [Co((^{13}C)Me(tren))$(NO_2)_2$]Cl was similarly prepared with (^{13}C)Me(tren).

[Co(Me(tren))Cl_2](ClO_4). Concentrated HCl (50 cm^3) was added to the brown filtrate above, or to solid [Co(Me(tren))$(NO_2)_2$]Cl, and the solution heated on a stream bath. NO_2 was evolved, and a blue solution was obtained. The latter was reduced to dryness and the blue residue ground to a fine powder and agitated with acetone. The filtered solid was then dissolved in the minimum amount of hot water and $LiClO_4$ immediately added, whence, on cooling in ice, blue crystals were obtained, which were filtered and dried in vacuo; yield 20 g (from brown mother liquor above). Anal. Calcd for $[CoC_7H_{20}Cl_2](ClO_4)$: Co, 15.13; C, 21.58; H, 5.18; N, 14.38; Cl, 27.30. Found: Co, 15.03; C, 22.0; H, 5.43; N, 14.39; Cl, 27.1. [Co((^{13}C)Me(tren))$(NO_2)_2$]Cl was treated identically to yield [Co((^{13}C)Me(tren))Cl_2](ClO_4). The blue solid gives a blue solution in water, which quickly (1 min) turns purple-red due to aquation of chloride. On addition of concentrated HCl the solution reverts to blue.

***t*-[Co(Me(tren))(NH_3)Cl]Cl_2 (Purple Isomer).** [Co(Me(tren))-Cl_2](ClO_4) was suspended in liquid NH_3 in an evaporating dish and the ammonia allowed to slowly evaporate by using a slow stream of air (fume cupboard). The remaining purple solid residue was washed with methanol, filtered (the red-brown filtrate was retained for further use), and then recrystallized from hot dilute HCl (0.1 mol dm^{-3}) by adding LiCl and cooling in ice. The resulting purple crystals were filtered off, washed with ethanol and ether, and dried in air (ϵ_{534} 139, ϵ_{368} 132 M^{-1} cm^{-1}). Anal. Calcd for $[Co(C_7H_{20}N_4)(NH_3)Cl]Cl_2$: Co, 17.21; C, 24.53; H, 6.17; N, 20.44; Cl, 31.05. Found: Co, 17.0; C, 24.44; H, 6.37; N, 20.4; Cl, 30.4. A sample was converted to the iodide salt by dissolving in H_2O and adding NaI to initiate crystallization. Cooling in ice yielded crystals, which were recrystallized from warm water. These were submitted for X-ray crystallography.

Resolution of *t*-[Co(Me(tren))(NH_3)Cl]Cl_2. *t*-[Co(Me(tren))-(NH_3)Cl]Cl_2 (0.86 g) was dissolved in the minimum volume of warm (50 °C) water and 1 equiv of Na_2((+)-$AsC_4H_2O_6)_2·2.5H_2O$ (0.77 g, $[\alpha]_{589}$ +21°) added. When the container was scratched, the diastereoisomer $(-)_{505}$-*t*-[Co(Me(tren))(NH_3)Cl]((+)-$AsC_4H_2O_6)_2·2H_2O$ slowly crystallized. This was recovered and recrystallized from warm water to constant optical rotation (0.3 g, $[\alpha]_{505}$ −288°). Anal. Calcd for $[Co(C_7H_{20}N_4)(NH_3)Cl](AsC_4H_2O_6)_2·2H_2O$: C, 24.13; H, 4.15; N, 9.38. Found: C, 23.5; H, 4.13; N, 8.4. Further fractions with lower rotations were isolated from the filtrate. $(-)_{505}$-*t*-[Co(Me-(tren))(NH_3)Cl]((+)-$AsC_4H_2O_6)_2·2H_2O$ (0.3 g) was dissolved in water (20 cm^3) at room temperature and one drop of concentrated HCl added. The solution was passed through a column of Dowex 1-X8 anion-exchange resin in the Cl^- form. The eluent was evaporated to low volume in vacuo without heating, and the complex crystallized from dilute HCl (0.15 g, $[\alpha]_{505}$ (−710°). Anal. Calcd for [Co-$(C_7H_{20}N_4)(NH_3)Cl]Cl_2·H_2O$: C, 23.34; H, 7.00; N, 19.45. Found: C, 23.3; H, 7.1; N, 19.3.

***anti-p*-[Co(Me(tren))(NH_3)Cl]$(ClO_4)_2$ or -$(ZnCl_4)$.** [Co(Me-(tren))Cl_2](ClO_4) was completely dissolved in liquid NH_3 (a few crystals NH_4Cl were added) and after standing overnight was taken to dryness with use of a stream of air. The residue was dissolved in the minimum volume of cold water and solid NaOH added. After 30 min the hydrolyzed reaction mixture was quenched with concentrated HCl and then evaporated to dryness with use of a steam bath. The resulting solid was dissolved in water (pH 3.5) and sorbed on to Dowex 50W-X2 resin (H^+ form), and the various products were separated and then eluted with 1.0 mol dm^{-3} HCl. The first purple band (chloro–aqua complex) was retained for further use. The second band (red) was collected and evaporated to dryness with use of a rotary evaporator (0.2 mmHg, 45 °C). The solid remaining was dissolved in the minimum volume of hot water (pH 3.5) and $NaClO_4·H_2O$ added with stirring and cooling. The fine red crystals that deposited were filtered, washed with ethanol and ether, and dried in air. The compound was recrystallized from hot water (pH 3.5) by adding $NaClO_4·H_2O$ and cooling (ϵ_{503} 104, ϵ_{370} 104 M^{-1} dm^3 cm^{-1}). Anal. Calcd for $[Co(C_7H_{20}N_4)(NH_3)Cl](ClO_4)_2$: C, 17.87; H, 4.93; N, 14.88; Cl, 22.60. Found: C, 17.98; H, 5.22; N, 14.68; Cl, 22.70. The purity was checked for each sample by ^{1}H NMR (see Results section). Samples of *anti-p*-[Co(Me(tren))(NH_3)Cl]$(ZnCl_4)$ were prepared by addition of a solution of $ZnCl_2$ in concentrated HCl to the material isolated from the ion-exchange column or to pure samples of the perchlorate salt dissolved in warm water. This salt was recrystallized from water (pH 3.5) by addition of a little concentrated HCl. Anal. Calcd for $[Co(C_7H_{20}N_4)(NH_3)Cl](ZnCl_4)$: C, 17.55; H, 4.84; N, 14.62; Cl, 37.02. Found: C, 17.66; H, 4.88; N, 14.68; Cl, 37.22. Crystals of this material were grown for X-ray crystallography from an aqueous solution containing a few drops of concentrated HCl. Purity was checked by ^{1}H NMR and ion-exchange chromatography.

Samples of [((^{13}C)Me(tren))(NH_3)Cl]$(ClO_4)_2$ were similarly prepared from [Co((^{13}C)Me(tren))Cl_2](ClO_4). Anal. Calcd for $[Co(C_7H_{20}N_4)(NH_3)Cl](ClO_4)_2$: C, 17.88; H, 4.93; N, 14.88; Cl, 22.60. Found: C, 17.90; H, 4.92; N, 14.87; Cl, 22.65.

Resolution of *anti-p*-[Co(Me(tren))(NH_3)Cl]$(ZnCl_4)$. *anti-p*-(*RS*)-[Co(Me(tren))(NH_3)Cl]$(ClO_4)_2$ (1 g) was dissolved in warm water (3 cm^3), and Na_2((+)-$AsC_4H_2O_6)_2·2.5H_2O$ (1.3 g, 2 equiv) was added. When the container was scratched at room temperature for 15 min, optically pure $(+)_{505}$-*anti-p*-(*S*)-[Co(Me(tren))(NH_3)Cl]-((+)-$AsC_4H_2O_6)_2$ slowly deposited as fine red crystals. These were washed with aqueous methanol and then absolute methanol and dried in air (0.77 g, $[\alpha]_{505}$ +285°). The filtrate was reserved to recover the *R* isomer (below). The $(+)_{505}$ diastereoisomer was dissolved in hot water (150 cm^3) and passed down a column of Dowex AG1-X4 resin (Cl^- form). The eluent was acidified with HCl and evaporated to dryness with a rotary evaporator (0.2 mmHg, 50 °C), and the residue was taken up in warm water (2 cm^3) and crystallized by addition of $ZnCl_2$ containing one drop of concentrated HCl. The red crystals were washed with ice-cold aqueous methanol and absolute methanol and air-dried (0.33 g, $[\alpha]_{505}$ + 410°). Anal. Calcd for $[Co(C_7H_{20}N_4)(NH_3)Cl](ZnCl_4)$: C, 17.55; H, 4.84; N, 14.62; Cl, 37.02. Found: C, 17.54; H, 4.51; N, 14.39; Cl, 37.31. A sample was crystallized slowly at room temperature from water acidified with HCl for X-ray crystallography.

The filtrate containing the *R* diastereoisomer (3.5 cm^3) was diluted with methanol (2 cm^3), whence, when the container was scratched, red crystals deposited. These were washed and dried as before (0.65 g, $[\alpha]_{505}$ −214°). The complex was converted to the chloride salt in solution and crystallized by addition of $ZnCl_2$ and HCl to give optically impure $(-)_{505}$-*anti-p*-(*R*)-[Co($C_7H_{20}N_4$)(NH_3)Cl]$(ZnCl_4)$ (0.3 g, $[\alpha]_{505}$ −330°). Anal. Found: C, 17.51; H, 4.93; N, 14.62.

***syn-p*-[Co(Me(tren))(NH_3)Cl]$(ClO_4)_2$.** A mixture of the red isomers obtained by treatment of [Co(Me(tren))Cl_2](ClO_4) with liquid NH_3 and subsequent alkaline hydrolysis and reanation (cf. above) was heated to dryness on a steam bath. Heating of the dry material was continued for 16 h. A dilute solution of the product was loaded onto a column of Dowex 50W-X2 resin (H^+ form) and eluted with 1 mol dm^{-3} HCl. This resulted in a purple band of [Co(Me-(tren))$(OH_2)Cl]^{2+}$ and two red bands of $[Co(Me(tren))(NH_3)Cl]^{2+}$. The slower moving red band (obtained in increased yield by prolonged heating of the solid) was taken from the column by removing that portion of resin containing it. The complex was eluted with 3–4 mol dm^{-3} HCl and taken to dryness in vacuo on a rotary evaporator (0.2 mmHg, 45 °C). The remaining solid was dissolved in the minimum volume of hot water and crystallized by adding $NaClO_4·H_2O$ with stirring and cooling. The crystals were removed, washed with ethanol and ether, and dried in air (ϵ_{507} 108, ϵ_{372} 107). Anal. Calcd for $[Co(C_7H_{20}N_4)(NH_3)Cl](ClO_4)_2$: C, 17.87; H, 4.93; N, 14.88; Cl, 22.60. Found: C, 17.95; H, 5.16; N, 14.83; Cl, 22.5. The compound was chromatographically pure, and the ^{1}H NMR spectrum showed only one methyl doublet (cf. Results section). A sample of *syn-p*-[Co(Me(tren))(NH_3)Cl]$(ZnCl_4)$ was obtained in the same manner by addition of $ZnCl_2$ in concentrated HCl to the concentrated aqueous eluate following extraction and concentration. Anal. Found: C, 17.51; H, 4.94; N, 14.51; Cl, 36.84. Crystals of this material were grown for X-ray crystallography from water at room temperature. *syn-p*-[Co((^{13}C)Me(tren))(NH_3)Cl]$(ClO_4)_2$ was obtained from [Co-

$((^{13}C)Me(tren))Cl_2](ClO_4)$ in the same way. Anal. Found: C, 17.99; H, 4.97; N, 14.87; Cl, 22.56.

***s*-[Co(Me(tren))(NH$_3$)Cl](ZnCl$_4$)·H$_2$O.** Unpurified samples of *syn-p*-$[Co(Me(tren))(NH_3)Cl]Cl_2$ obtained by ion-exchange chromatography as above were evaporated to dryness in vacuo and redissolved (5 g) in 2 mol dm^{-3} HCl to give a less than saturated solution. This solution was left to stand at room temperature for 24 h before sorbing on Dowex 50W-X2 resin (H^+ form) contained in a 60 × 10 cm column. Slow elution with 1 mol dm^{-3} HCl was continued to the end of the column (30 h). Initially two red bands separated, and then the first band spread on further elution. The "tail" portion of this first band was recovered by removing that portion of resin containing it and eluting with 6 mol dm^{-3} HCl. The eluate was evaporated to dryness on a rotary evaporator (0.2 mmHg, 50 °C). ^{1}H NMR in 0.5 mol dm^{-3} DCl showed large amounts of the *s* isomer contaminated with 10–30% of the anti-*p* isomer. Pure *s*-$[Co(Me(tren))(NH_3)Cl](ZnCl_4)\cdot H_2O$ was obtained by fractional crystallization from hot water (pH 3.5) following addition of a little $ZnCl_2$ in concentrated HCl. The crystals obtained in the first one or two fractions were washed with ethanol and ether and air-dried. The combined fractions of pure *s* isomer (^{1}H NMR) were recrystallized from hot water (yield from 5 g of crude syn-*p* isomer ca. 2.2 g; ϵ_{511} 83, ϵ_{370} 86). Anal. Calcd for $[Co(C_7H_{20}N_4)(NH_3)Cl](ZnCl_4)\cdot H_2O$: C, 16.92; H, 5.07; N, 14.09; Cl, 35.67. Found: C, 17.15; H, 5.16; N, 14.14; Cl, 35.74. Crystals for X-ray crystallography were grown slowly from water at room temperature. The remaining material was converted to the perchlorate salt by passing a dilute solution down a column of Dowex AG1-X4 resin (ClO_4^- form), evaporating to dryness in vacuo, and crystallizing from water by adding $NaClO_4\cdot H_2O$. The crystals that formed on cooling were removed, washed with ethanol and ether, and dried in air. A further crystallization yielded pure *s*-$[Co(Me(tren))(NH_3)Cl](ClO_4)_2$. Anal. Found: C, 17.50; H, 5.21; N, 14.64; Cl, 22.83. All samples were checked for isomeric purity by ^{1}H NMR in 0.5 mol dm^{-3} DCl.

s-$[Co((^{13}C)Me(tren))(NH_3)Cl](ClO_4)_2$ was prepared from crude *syn-p*-$[Co((^{13}C)Me(tren))(NH_3)Cl]Cl_2$ in the same manner.

***anti-p*-[Co(Me(tren))(NH$_3$)Br](ClO$_4$)$_2$.** *anti-p*-$[Co(Me(tren))(NH_3)Cl](ClO_4)_2$ (2 g) dissolved in water (50 cm^3) was base hydrolyzed at pH 8.0 (pH stat, 0.1 mol dm^{-3} LiOH, 2 min) and passed through a short anion-exchange column (Dowex 1-X4, Br^- form), and the eluant was quenched with concentrated HBr (7.6 mol dm^{-3}, 5 cm^3) and taken to dryness on a rotary evaporator. The residue was twice treated with concentrated HBr and taken to dryness on a steam bath. The remaining solid was dissolved in water, loaded onto Dowex 50W-X2 resin (H^+ form, 8–10 cm long) and eluted with 1 mol dm^{-3} HBr. The first red-purple band was collected and taken to dryness on a rotary evaporator, and the solid was taken up in the minimum volume of warm water and $NaClO_4\cdot H_2O$ added with scratching and cooling. The dark red crystals were removed, washed with ethanol, and dried in air. The complex was recrystallized from hot water (pH 3.5) by adding $NaClO_4\cdot H_2O$ and cooling (ϵ_{541} 145 M^{-1} dm^3 cm^{-1}). Anal. Calcd for $[Co(C_7H_{20}N_4)(NH_3)Br](ClO_4)_2$: C, 16.32; H, 4.50; N, 13.60. Found: C, 16.3; H, 4.7; N, 13.4.

***syn-p*-[Co(Me(tren))(NH$_3$)Br](ClO$_4$)$_2$·H$_2$O.** *syn-p*-$[Co(Me(tren))(NH_3)Cl](ClO_4)_2$ (2.3 g) in warm water (20 cm^3) was treated at ~30 °C with $AgClO_4$ (2.1 g). After 1 h aqueous concentrated HBr (5 cm^3, 7.6 mol dm^{-3}) was added and the mixture filtered through a Hyflo-protected sintered filter, and the filtrate and washings were taken to dryness on a rotary evaporator. The residue was twice treated with concentrated HBr and taken to dryness on a steam bath. The remaining solid was dissolved in water, loaded on to Dowex 50W-X2 resin (H^+ form, 10 cm long) and eluted with 1 mol dm^{-3} HBr. The second red-purple band (50–60%) when well separated from the first band was removed from the column by carefully removing the resin, and the complex was eluted by washing with ~3 mol dm^{-3} HBr. The acidity was reduced by treating the filtrate with AG3-X4 (CO_3^{2-} form) exchange resin and the complex precipitated by adding a solution of sodium tetraphenylborate. The pink, voluminous precipitate was filtered, washed with water, and then treated with concentrated HBr (5 cm^3). The crude bromide salt crystallized on cooling and adding isopropyl alcohol. It was collected and washed with MeOH and dried in air. The complex was recrystallized from warm water by adding $NaClO_4\cdot H_2O$ to the concentrated, filtered solution and cooling in an ice bath. Anal. Calcd for $[Co(C_7H_{20}N_4)(NH_3)Br](ClO_4)_2\cdot H_2O$: C, 15.77; H, 4.73; N, 13.14. Found: C, 15.8; H, 4.7; N, 13.1. Found: C, 15.8; H, 4.7; N, 13.1.

***s*-[Co(Me(tren))(NH$_3$)Br](ClO$_4$)$_2$.** The first band that separated on the ion-exchange column during the above preparation of the syn-*p* isomer was extracted with ~3 mol dm^{-3} HBr and the acidity reduced by treating with AG3-X4 (CO_3^{2-} form) anion-exchange resin, and the complex precipitated as the insoluble tetraphenylborate salt as described above. When the complex was treated with concentrated HBr and cooled in ice, the crude product crystallized (apparently the anti-*p* bromo isomer also present did not survive the treatment with the CO_3^{2-} resin or was more soluble). The crude product was recrystallized as the perchlorate salt as outlined above for the *s* isomer. Anal. Found: C, 15.7; H, 4.8; N, 13.0.

***anti-p*- and *s*-[Co(Me(tren))(NH$_3$)N$_3$](ClO$_4$)$_2$·H$_2$O.** To a mixture of the three isomeric chloro isomers (4 g) dissolved in water (25 cm^3) was added LiN_3 (5 g, ca. 4 mol dm^{-3}) and base hydrolysis allowed to continue for 30 min (pH ~8). The solution was then diluted to ca. 1.0 dm^3, loaded on to Dowex cation-exchange resin, and eluted in the dark with 1.0 mol dm^{-3} HCl. After the first band had traveled about 40 cm, the resin containing it was removed and divided into the front-running portion and the trailing portion. These were separately eluted with use of a glass filter with ca. 2.0 mol dm^{-3} HCl, and the solutions were neutralized with AG3-X4 (CO_3^{2-} form) anion-exchange resin and reduced in volume to ca. 10 cm^3. When $NaClO_4$ was added and the solution was cooled, the red-black azido complexes crystallized. These were removed and washed with aqueous ethanol and then ether. They were recrystallized to NMR purity (single ^{1}H doublets) from warm water by adding $NaClO_4$. About 0.2 g of the anti-*p* isomer and ~70 mg of the *s* isomer were obtained. Anal. Calcd for the anti-*p* isomer: C, 16.98; H, 5.09; N, 22.63. Found: C, 17.0; H, 5.2; N, 22.4.

***syn-p*-[Co(Me(tren))(NH$_3$)N$_3$](ClO$_4$)$_2$·1.5H$_2$O.** The second red-purple band from the above separation was similarly removed from the resin, treated with AG3-X4 resin, and reduced in volume to ~7 cm^3. Addition of $NaClO_4$ and cooling in an ice bath resulted in a small amount of the dark *s*-$[Co(Me(tren))(NH_3)N_3](ClO_4)_2$ salt crystallizing. This was recrystallized carefully from the minimum volume of warm water by adding $NaClO_4$, filtering, and cooling. It was washed with aqueous isopropyl alcohol and then ether. It was shown to be isomerically pure by ^{1}H NMR.

***anti-p*- and *s*-[Co(Me(tren))(NH$_3$)$_2$](ClO$_4$)$_3$.** These were prepared and characterized as described previously[3] with the 9.6% ^{13}C-enriched Me(tren).

NMR Spectra and Product Distribution. ^{1}H NMR spectra were obtained with JEOL MH-100 and/or Varian HA-100 spectrometers in Me_2SO-d_6 or 0.1 mol dm^{-3} DCl solvents with *tert*-butyl alcohol as an internal reference. In some cases (0.1 mol dm^{-3} DCl) D_2SO_4 (98%) was added to move the HOD signal downfield away from the N–H signals. Homonuclear spin decoupling of protons was carried out on the Varian HA-100 spectrometer in the frequency sweep mode with a Hewlett-Packard 4204A audio oscillator. Proton exchange was followed at 25 °C with use of D_2O buffers. The complex ([Co] = 0.1–0.2 mol dm^{-3}) was dissolved in the buffer (0.5 cm^3) and the disappearance of the N–H signal, or the collapse of the CH_3 doublet, followed as a function of time.

^{13}C spectra were obtained with a JEOL FX-60 pulsed spectrometer operating at 15.1 MHz in the Fourier transform mode (noise decoupling of protons, 5-W power). Solutions were prepared in D_2O, D_2O–DCl, or D_2O–NaOD, and the spectrometer was locked on D_2O (offset ca. 36.5 kHz). Chemical shifts were measured from the lock signal, or from a dioxane internal standard, and referenced to tetramethylsilane. Typically a 1000-Hz spectral width was examined with use of 4K data points and single 45° pulses with 9-μs width and a 1.2- or 3-s repetition time. Natural-abundance ^{13}C samples required ca. 25K scans per spectrum, but samples containing 9.6 or 30% *N*-(^{13}C)methyl gave suitable methyl signals after 80–100 scans (1.2-s repetition time). Temperature was maintained at 20 (±2) °C with a stream of air through the sample compartment. Product distributions for the induced aquation and base hydrolysis experiments were determined with both ^{1}H and ^{13}C NMR data. Both integrated (^{1}H, 100 MHz Varian instrument, ~26 °C) and pulsed (FX-60: ^{13}C, 100 pulses, 1.25 s/pulse; ^{1}H, 15–20 pulses, 4.2 s/pulse, ~20 °C) data were used. Results with prepared standard mixtures were in agreement with the known distributions.

Aquation. Aquation of the three red $[Co(Me(tren))(NH_3)Cl]^{2+}$ isomers was followed spectrophotometrically (Gilford 2400) at 25 ± 0.05 °C, I = 1.0 mol dm^{-3} ($NaClO_4$), and [Co] = (2–9) × 10^{-3} mol dm^{-3}. The complex (50 mg) in dilute $HClO_4$ (100 cm^3, 10^{-3} mol dm^{-3})

Table I

	anti-p-(*RS*)-[Co(Me(tren))NH_3Cl]-($ZnCl_4$) (racemate)	*anti-p*-(*S*)-λλδ-[Co(Me(tren))NH_3Cl]-($ZnCl_4$) (optically active form)	*s*-(*RS*)-[Co(Me(tren))NH_3Cl]-($ZnCl_4$)·H_2O (racemate)
(a) Crystal Data ($C_7H_{23}Cl_5CoN_5Zn$, M_r = 478.86, $F(000)$ = 968, T = 21 °C)			
a, Å	12.850 (1)	11.681 (1)	13.770 (1)
b, Å	11.754 (1)	16.717 (1)	12.265 (1)
c, Å	11.863 (1)	9.195 (1)	10.613 (1)
β, deg	96.41 (1)	90	92.72 (2)
V, Å^3	1780.5 (5)	1795.5 (5)	1790.3 (6)
D_m, g cm^{-3}	1.77	1.76	1.81
D_c, g cm^{-3}	1.785	1.771	1.843
Z	4	4	4
space group	$P2_1/c$	$P2_12_12_1$	$P2_1/n$
μ, cm^{-1}	160.7	159.4	160.5
cryst size, mm	0.24 × 0.05 × 0.03	0.23 × 0.09 × 0.08	0.20 × 0.04 × 0.04
transmission factors for F_o (Cu Kα radiation)			
min	0.556	0.451	0.660
max	0.779	0.628	0.764
av	0.713	0.574	0.744
(b) Structural Statistics			
no. of reflctns			
total (to 126° 2θ)	3303	3348	3336
$>3\sigma(I)$	2181 (66%)	2574 (77%)	1602 (48%)
unique $>3\sigma(I)$	1989	2292	1424
$R_s = \Sigma\sigma(F_o)/\Sigma F_o$	0.031	0.031	0.044
final *R*	0.038	0.038	0.053
final R_w	0.044	0.044	0.057
$[\Sigma w(\lvert F_o - F_c\rvert)^2/(m-n)]^{1/2}$ [a]	1.27	1.30	1.45

[a] Where *m* is the number of observations and *n* is the number of parameters varied.

was maintained at 25 °C for 50 h ($t_{1/2}$ = 10 h for the syn-*p* isomer). $AgClO_4$ was then added in excess to precipitate Cl^- and the solution filtered and evaporated to dryness in vacuo without heating. The residue was dissolved in 0.1 mol dm^{-3} $DClO_4$ (0.4 cm^3) and filtered and the ^{1}H NMR recorded. The product distribution was determined from the integrated signals due to the *N*-methyl protons and the stereochemistries from the chemical shifts relative to *tert*-butyl alcohol.

Base Hydrolysis. Rate data for the three chloro isomers were obtained spectrophotometrically at 25.00 ± 0.05 °C in 0.1 mol dm^{-3} MES, HEPES, Tris, or glycine buffers with use of rapid-mixing (Cary 16 K) or stopped-flow (Durrum-Gibson) techniques. The ionic strength was maintained at 1.0 mol dm^{-3} with $NaClO_4$ ([Co] = (7.6–22) × 10^{-4} mol dm^{-3}). pH measurements were carried out with Radiometer equipment, pH meter TTTIC with a scale expander, type PHA630T, glass electrode, type G202B, and a saturated calomel electrode reference. For perchlorate buffers a salt bridge (1.6 mol dm^{-3} NH_4NO_3, 0.2 mol dm^{-3} $NaNO_3$ (pH 7)) was used to protect the calomel electrode. The pH of D_2O buffers was similarly measured and the empirical conversion[12] pD = pH + 0.4 applied to evaluate [D^+]. The buffer capacities of all solutions were checked by measurement of pH before and after reaction.

Product analyses for base hydrolyses were obtained from ^{13}C NMR with use of peak intensities as a measure of relative concentrations. The complexes [Co((^{13}C)Me(tren))(NH_3)X](ClO_4)$_2$ (X = Cl, Br, NH_3) (200 mg) were dissolved in 2.0 mol dm^{-3} NaOD solutions in D_2O (1 cm^3), and the changes in intensities were monitored as a function of time. Spectral data were collected for 100 scans and recorded at various time intervals. Examination of the kinetics of isomerization in the hydroxo complexes allowed estimates of the product distribution from base hydrolysis.

Induced aquation by Hg^{2+} ions was followed spectrophotometrically (Cary 16 K) at 25 ± 0.05 °C and initiated by rapid mixing of complex solutions in 1.0 mol dm^{-3} $NaClO_4$ with an equal volume of $Hg(ClO_4)_2$ in perchloric acid, I = 1.0 mol dm^{-3} ($NaClO_4$) ([Co] = (5–16) × 10^{-4} mol dm^{-3}). Product analysis was by ^{1}H and ^{13}C NMR with use of integrated signals or peak heights. The complex (75 mg, perchlorate salt) was dissolved in a solution of 1 mol dm^{-3} $Hg(ClO_4)_2$ in $DClO_4$ (0.4 cm^3, pD 1.4) and the ^{1}H spectrum recorded immediately and then repeated at intervals over several hours. The procedure for ^{13}C NMR was the same, with [Co((^{13}C)Me(tren))(NH_3)Cl](ClO_4)$_2$ (200 mg) in 1 cm^3 of solution. Data collection required ca. 300 scans (pulse repetition 1.2 s). The products of Ag^+-induced aquation were also investigated. Samples (200 mg, ^{13}C enriched) were dissolved in 2.5 mol dm^{-3} $AgClO_4$ in 0.11 mol dm^{-3} $DClO_4$ (1.0 cm^3) and allowed to react to completion (30, 5, and 10 min, respectively, for the anti-*p*, syn-*p*, and *s* isomers). The solutions were filtered into the NMR tubes and ^{13}C (FX-60) and ^{1}H (MH100) spectra recorded. Spectra were also recorded on the Varian HA100 spectrometer of normal-abundance samples (90 mg) with use of 0.5 cm^3 of solution.

Equilibrium Measurements. (A) Chloro Isomers. Samples of the three red [Co(Me(tren))(NH_3)Cl]Cl_2 complexes were eluted from the Dowex 50W-X2 resin with HCl and taken to dryness on a rotary evaporator (^{1}H NMR showed little isomerization). The residues were dissolved in 1.0 or 2.0 mol dm^{-3} HCl (1.0 cm^3, [Co] ≈ 0.1 mol dm^{-3}) and maintained at 25, 40, and 80 °C until equilibration was complete (1–5 days). The solutions were then freeze-dried and redissolved in 1 mol dm^{-3} DCl (0.4 cm^3) and ^{1}H spectra recorded. Relative concentrations were estimated from heights of the CH_3 doublets (100 MHz; 1.23, 1.10, and 0.97 ppm with respect to *tert*-butyl alcohol).

(B) Aqua Isomers. Samples of the three chloro complexes (ca. 50 mg) in ca. 2.0 mol dm^{-3} Hg^{2+}–$DClO_4$–D_2O (0.5 cm^3) were allowed to react and then filtered into NMR tubes and the ^{13}C and ^{1}H spectra recorded as a function of time (26 ± 1 °C). Similar data were recorded after ca. 40 min following treatment with $AgClO_4$–$DClO_4$–D_2O.

(C) Hydroxo Isomers. Samples of the three chloro isomers (ca. 40 mg) were treated with 1.0 or 2.0 mol dm^{-3} NaOD, and the ^{13}C spectra recorded as a function of time. The ^{1}H spectra of the hydroxo and the $DClO_4$-neutralized aqua products were recorded when equilibrium had been reached.

Crystallography. X-ray data were collected on three crystals, the *anti-p*-(*RS*)-[Co(Me(tren))(NH_3)Cl]($ZnCl_4$) racemate, the (+)$_{505}$-*anti-p*-(*S*)-[Co(Me(tren))(NH_3)Cl]($ZnCl_4$) optical isomer ([α]$_{505}$ +410°), and the *s*-(*RS*)-[Co(Me(tren))(NH_3)Cl]($ZnCl_4$)·H_2O racemate. Cell dimensions were obtained by least-squares refinements of the setting angles of 12 carefully centered reflections having 2θ values between 90 and 120° on a Picker FACS-1 automatic four-circle diffractometer with graphite-monochromated Cu $K\alpha_1$ radiation (λ = 1.540 51 Å). Crystal data for all three structures are given in Table Ia.

Intensity data were collected by the θ–2θ continuous-scan technique with use of a scan speed of 2° min^{-1} and a scan range from (2θ − 0.9) to (2θ + 0.9 + Δ)°, where Δ is the 2θ separation (in degrees) of the Cu $K\alpha_1$ and $K\alpha_2$ peaks for the reflection concerned. Stationary-

(12) P. K. Glascoe and F. A. Long, *J. Phys. Chem.*, **64**, 188 (1960).

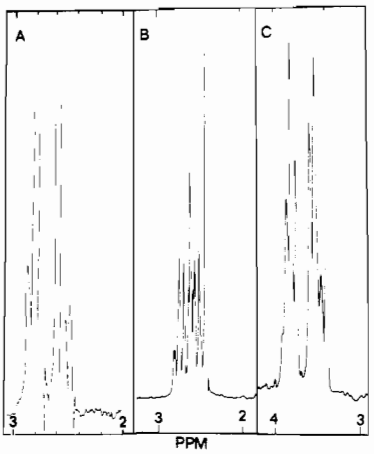

Figure 1. ^1H NMR spectra (100 MHz) of (A) tren in $CDCl_3$ (internal Me_4Si), (B) Me(tren) in $CDCl_3$ (internal Me_4Si), and (C) Me(tren)·3HCl in D_2O (external Me_4Si).

background counts of 10 s duration were made at each extreme of the scan range. The intensities of three standard reflections monitored during each data collection did not vary significantly. Intensities were collected for reflections with 2θ (Cu Kα) values in the range 3–126°. In each case a value of 0.04 was used for the experimental uncertainty factor p.[13,14] Intensities were corrected for Lorentz and polarization effects and later for absorption by the analytical method of De Meulenauer and Tompa.[15]

Each structure was solved by the direct-methods program MULTAN[16] and refined to convergence by full-matrix least squares. Atomic scattering factors and anomalous dispersion values were taken from ref 17. After all nonhydrogen atoms had been included and refined, resulting difference maps indicated all hydrogen positions. The final scattering model in each case was one in which all nonhydrogen atoms were refined with anisotropic thermal parameters and the hydrogen atoms were treated as fixed-atom contributors. The adequacy of the weighting scheme was indicated by an analysis of $w(|F_o| - |F_c|)$ vs. F_o and $(\sin\theta)/\lambda$, where $w = 1/\sigma^2(F)$. There were no peaks significantly higher than background in the final difference map. Further details of data collection and structure refinement are given in Table Ib. Final atomic orthogonalized parameters are listed in Table V and the atomic (fractional) and thermal parameters in Table XIII (supplementary material).

Strain Energy Minimization Calculations. The method was the same as that described in detail for β-$[Co(trien)(glyO)]^{2+}$,[18] and the force field parameters were the same as those used for the $[Co(tren)(NH_3)Cl]^{2+}$ study.[9] In each case the final geometry and energy were identical in starting from the "crystal" configuration and from the minimized p-$[Co(tren)(NH_3)Cl]^{2+}$ configuration[9] in which N–H had been replaced by N–CH_3 (1.500 Å). Energy minimization was achieved in 10 or less iterations by appropriate use of the damping factor. Detailed nonbonded and torsion-angle contributions (>0.4 kcal mol^{-1}) are given as part of Table VI, and a summary of the separate contributions to the strain energy are listed in Table VII.

Results and Discussion

1. Preparation and Properties of 2-(Methylamino)-2′,2″-diaminotriethylamine (Me(tren)). The ligand was prepared by condensing phthalimido-protected diethylenetriamine with (phenylsulfonyl)aziridine in refluxing acetonitrile (eq 1) followed by addition of methyl iodide (30% or 9.6% ^{13}C enriched for the enriched ligand) to a dimethylformamide solution in the presence of anhydrous sodium carbonate. The protecting groups were removed by refluxing in concentrated hydrochloric acid and the free base recovered by addition of solid KOH (eq 2). Since we had considerable trouble in obtaining a high-yield synthetic procedure and in ensuring the product was not contaminated with the unsubstituted material, the ^1H NMR spectra were taken and are reproduced in Figure 1. Me(tren)·3HCl could be obtained as a white powder from methanol by bubbling in HCl gas, although the neat ligand was used in most instances.

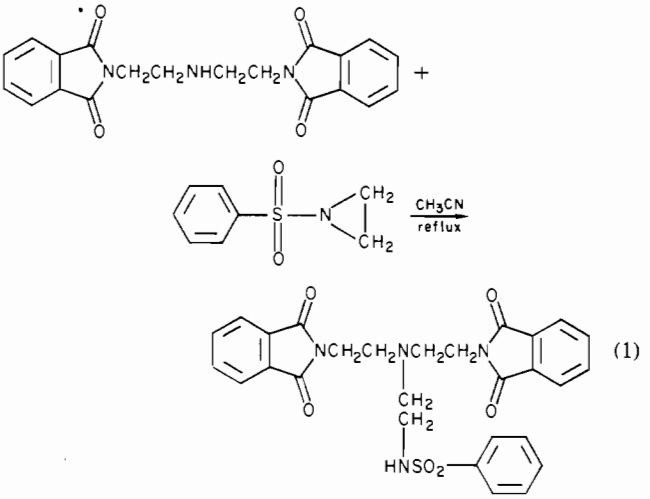

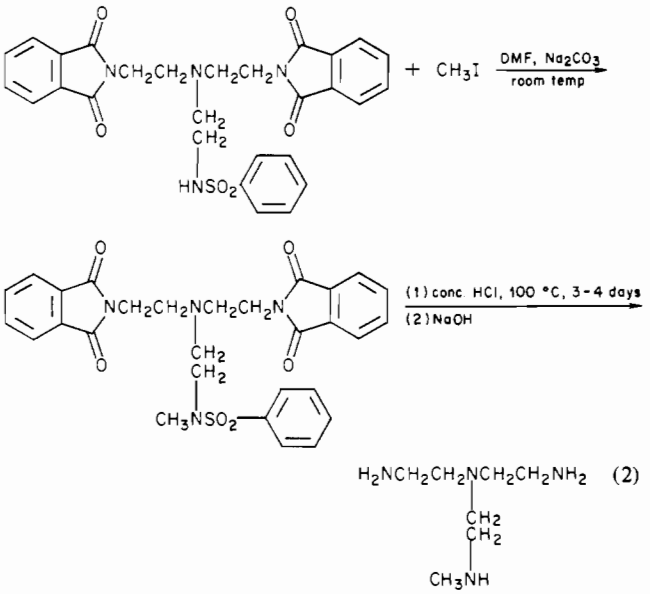

2. Preparation and Properties of Cobalt(III) Complexes. (A) $[Co(Me(tren))(NO_2)_2]Cl$. The initial complex was prepared from cobalt(II) chloride, Me(tren), and $NaNO_2$ by a procedure identical with that used by Collman, Kimura, and Young for the unsubstituted complex[22] (eq 3). Our experience

$$Co^{2+} + Me(tren) + 2NO_2^- + {}^1/_4O_2 + H^+ \rightarrow [Co(Me(tren))(NO_2)_2]^+ + {}^1/_2H_2O \quad (3)$$

is that this method is to be preferred over that via the μ-peroxo complex[9] and in general is to be preferred for similar tetradentate amine ligands. The crystallized product and the supernatant residues appear to be one isomer. The complex

(13) W. R. Busing and H. A. Levy, *J. Chem. Phys.*, **26**, 563 (1957).
(14) P. W. R. Corfield, R. J. Doedens, and J. A. Ibers, *Inorg. Chem.*, **6**, 197 (1967).
(15) J. De Meulenauer and H. Tompa, *Acta Crystallogr.*, **19**, 1014 (1965).
(16) J. P. Declerq, G. Germain, P. Main, and M. M. Wolfson, *Acta Crystallogr., Sect. A*, **A29**, 231 (1973).
(17) "International Tables for X-Ray Crystallography", Vol. IV, Kynoch Press, Birmingham, England, 1974.
(18) D. A. Buckingham, P. J. Cresswell, R. J. Dellaca, M. Dwyer, G. J. Gainsford, L. G. Marzilli, I. E. Maxwell, W. T. Robinson, A. M. Sargeson, and K. R. T. Turnbull, *J. Am. Chem. Soc.*, **96**, 1713 (1974).
(19) I. Olovsson and P. Jonsson, "The Hydrogen Bond", Vol. II, North-Holland Publishing Co., Amsterdam, 1976, p 395.
(20) L. Pauling, "The Nature of the Chemical Bond", Cornell University Press, Ithaca, New York, 1960.
(21) W. H. Baur, *Acta Crystallogr., Sect. B*, **B28**, 1456 (1972).
(22) J. P. Collman, E. Kimura, and S. Young, *Inorg. Chem.*, **9**, 1183 (1969).
(23) H. S. Harned and W. J. Hamer, *J. Am. Chem. Soc.*, **55**, 2194 (1933); W. F. K. Wynne-Jones, *Trans. Faraday Soc.*, **32**, 1397 (1936).

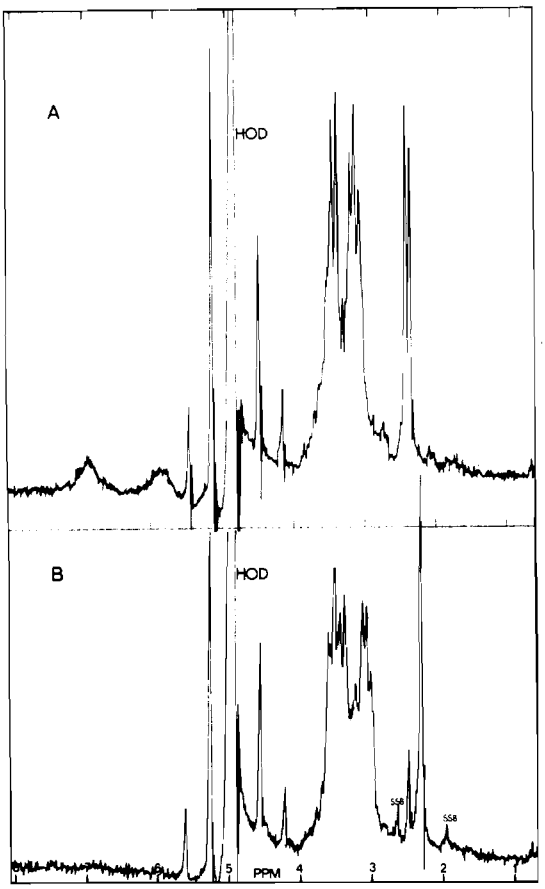

Figure 2. ^{1}H NMR spectra (100 MHz) of (A) [Co(Me(tren))-$(NO_2)_2$]Cl in D_2O (NaTPS standard) and (B) a mutarotated sample of the complex in part A in pH 10.5 buffer after 30 min. The singlet at 2.48 ppm (minor) represents the original compound and that at 2.28 ppm (major) a mutarotated isomer.

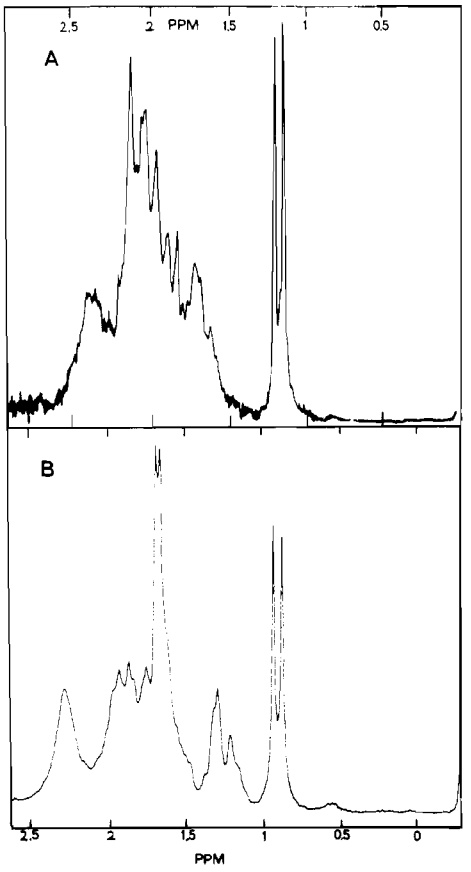

Figure 3. ^{1}H NMR spectra (100 MHz) of (A) *t*-[Co(Me(tren))-$(NH_3)Cl]Cl_2$ ("purple" isomer) in 10^{-3} mol dm^{-3} DCl (*tert*-butyl alcohol reference (1.36 ppm)) and (B) *t*-$[Co(Me(tren))(NH_3)OH_2]^{3+}$ prepared by treating the complex in part A with Hg^{2+} in 0.1 mol dm^{-3} $DClO_4$ (*tert*-butyl alcohol reference).

moves as a single band on ion-exchange chromatography (Dowex 50W-X2, 0.5 mol dm^{-3} $NaClO_4$) and shows only one methyl doublet (2.48 ppm, J = 6 Hz) in the ^{1}H NMR (Figure 2A). H exchange can be followed in neutral D_2O solutions ($t_{1/2} \simeq$ 30 min, pD 6.35), and one singlet (2.48 ppm) results. At higher pHs a new singlet slowly appears at higher field (2.28 ppm), and at equilibrium the two signals have an intensity ratio of 6 (2.28 ppm):1 (2.48 ppm) (Figure 2B). This mixture separates as two yellow bands on chromatography (Dowex 50W-X2, 0.5 mol dm^{-3} $NaClO_4$, pH ~5) with the minor band being the same as that found for the preparative material. These results imply mutarotation at the *N*-methyl center with the preparative material being less stable thermodynamically than the mutarotated product. It also requires the two isomers to be the syn and anti forms, although we cannot at this time state which is which.

(B) [Co(Me(tren))Cl_2]Cl. Four sets of doublets occur in the ^{1}H NMR (DCl solutions). These have been assigned as follows (ppm from NaTPS): 2.25, $[Co(Me(tren))Cl(H_2O)]^{2+}$ (minor isomer); 2.36, $[Co(Me(tren))Cl_2]^+$ (minor isomer); 2.58, $[Co(Me(tren))Cl_2]^+$ (major isomer); 2.63, $[Co(Me(tren))Cl(H_2O)]^{2+}$ (major isomer). The existence of two isomers was verified by the ^{13}C spectrum (30% $^{13}CH_3$-enriched complex), which showed methyl resonances 421.39 and 443.36 Hz downfield from dioxane. Treatment with $Hg(ClO_4)_2$ (0.1 mol dm^{-3} $DClO_4$) gave two sets of doublets in the ^{1}H spectrum (2.23 ppm (minor), 2.68 ppm (major)) with the high-field doublet rapidly undergoing H–D exchange to give a singlet. The relative intensities of the resonances for these diaqua complexes suggested that the induced aquation reaction produces more of the high-field isomer over that already present in the starting complex.

(C) (±)-[Co(Me(tren))$(NH_3)Cl]Cl_2$ (Purple Isomer). Treatment of $[Co(Me(tren))Cl_2]ClO_4$ with liquid NH_3 in an open evaporating dish results in the rapid formation of this complex as a purple methanol-insoluble material (repeated treatment with liquid NH_3, or treatment in an enclosed Dewar flask, results in $[Co(Me(tren))(NH_3)_2](ClO_4)_3$; cf. ref 3). The complex chromatographed as a single band on Dowex 50W-X2 cation-exchange resin (1.0 mol dm^{-3} HCl), and only one doublet occurred in the ^{1}H NMR spectrum (2.53 ppm, 10^{-3} mol dm^{-3} DCl, Figure 3A). Seven distinguishable carbons were found in the ^{13}C NMR. Treatment with $Hg(NO_3)_2$ or $AgClO_4$ or standing in 10^{-3} mol dm^{-3} $HClO_4$ (3 months) gave the corresponding *t*-aqua complex (doublet at 2.55 ppm, Figure 3B), and reanation with aqueous HCl gave a quantitative recovery of the *t*-chloro complex. However if the *t*-chloro complex was allowed to stand at 40 °C for 8 days, pH 10, rearrangement to a mixture of the three red *p* isomers occurred. This was verified by reanation with hydrochloric acid and separation on the Dowex cation-exchange resin (1.0 mol dm^{-3} HCl). Similarly, base hydrolysis in 1.0 mol dm^{-3} NaOH (10 min, 25 °C) followed by reanation gave the three red *p*-$[Co(Me(tren))(NH_3)Cl]^{2+}$ isomers together with some *t*-$[Co(Me(tren))(H_2O)Cl]^{2+}$. The latter complex reverted to *t*-$[Co(Me(tren))Cl_2]Cl$ on evaporation to dryness (^{1}H NMR). In this respect the *t*-$[Co(Me(tren))(NH_3)Cl]^{2+}$ ion differs from the unsubstituted *t*-$[Co(tren)(NH_3)Cl]^{2+}$ species, which gives ~15% of the *t*-$[Co(tren)(NH_3)OH]^{2+}$ ion together with 85% of the *p*-hydroxo complex on base hydrolysis.[9] In the present instance some base hydrolysis of NH_3 occurs probably as a reaction subsequent to base hydrolysis of chloride.[3] Treatment of the *t*-aminochloro complex with activated charcoal (3 days, 22 °C, "Norite" C) yielded only starting material and the

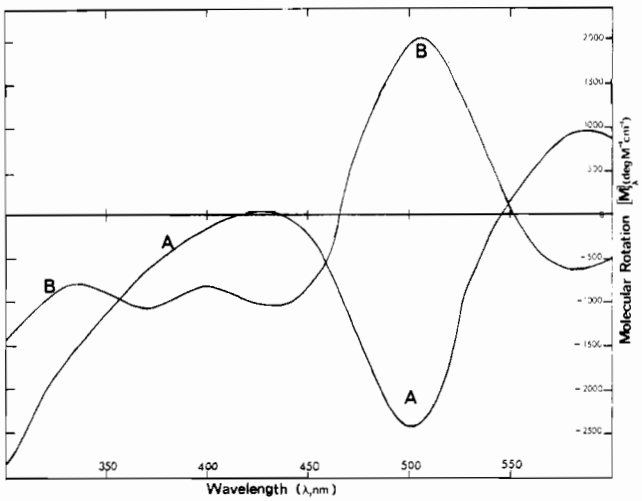

Figure 4. Optical rotatory dispersion curves for (A) $(-)_{505}$-*t*-$[Co(Me(tren))(NH_3)Cl]Cl_2 \cdot H_2O$ and (B) $(+)_{505}$-*anti*-*p*-(*S*)-$[Co(Me(tren))(NH_3)Cl](ZnCl_4)$, both in 10^{-3} mol dm^{-3} $HClO_4$.

t-aqua ion (reanation, aqueous HCl, ^1H NMR); no isomerization to the *p* isomers was detected.

Resolution of this complex was achieved through the arsenyl-(+)-tartrate diastereoisomer $(-)_{505}$-*t*-$[Co(Me(tren))(NH_3)Cl]((+)\text{-}AsC_4H_2O_6)_2$, and the optically pure complex was recrystallized as the monohydrate, $(-)_{505}$-*t*-$[Co(Me(tren))(NH_3)Cl]Cl_2 \cdot H_2O$ ($[\alpha]_{505}$ −710°). The ORD spectrum is reproduced in Figure 4A: $[M]_{589}$ 830°, $[M]_{505}$ −2430°.

Base hydrolysis was slow compared to that for the *p* isomers with $k_{obsd} = 2.2 \times 10^{-3}$ s^{-1} in 0.1 mol dm^{-3} glycine buffer at pH 10.0, 25 °C, and $\mu = 1.0$ ($NaClO_4$). This gives $k_{OH} = k_{obsd}/[OH^-] = 13$ mol^{-1} dm^3 s^{-1}, which is some 10^3 times slower than that for the *p* isomers (cf. Table X). A similar situation was found for the unsubstituted "tren" complexes[4,9] although the values of the rate constants in the present instance are some 10^2 times greater.

(D) *anti*-*p*-, *syn*-*p*-, and *s*-$[Co(Me(tren))(NH_3)Cl]Cl_2$ (Red Isomers). The so called "red" isomers[9] can be prepared via the μ-peroxo-decammine complex, as for the unsubstituted species,[9] or via the base hydrolysis of *t*-$[Co(Me(tren))(NH_3)Cl]Cl_2$ followed by reanation with aqueous HCl (see above). However, we found the most efficient method for large-scale preparation was via the diammine $[Co(Me(tren))(NH_3)_2]Cl_3$ and base hydrolysis of the *p*-ammine ligand. This results in a clean product,[3] and following reanation with aqueous HCl the three "red" chloro isomers can be directly separated by column chromatography (1.0 mol dm^{-3} HCl, Dowex 50W-X2 cation resin). Large columns (80 cm × 8 cm) were employed, and elutions were run continuously. Two red bands separated early on, with the slower moving being the syn-*p* isomer. The anti-*p* isomer was recovered from the larger front-end portion of the first band and the *s* isomer from the tail-end fractions. Recrystallizations of the product from the latter fractions were especially necessary, and in all cases purity was monitored by ^1H NMR; Figure 5A shows a nonequilibrium distribution of the three chloro isomers, *s* (2.32 ppm), anti-*p* (2.42), and syn-*p* (2.52). The distribution at equilibrium was investigated in some detail, and some results are given in Table II. At the HCl concentrations used no (<5%) aqua complexes were observed although the isomerization presumably occurs via an aquation–anation process. ^1H and ^{13}C spectra for the equilibrium mixture at 25 °C are given by Figure 5, parts B and C, respectively. Product distribution data was obtained from the heights of the methyl doublets. At 25 °C these give K_{21} = [syn-*p*]:[anti-*p*] = 0.13 (±0.01) and K_{31} = [*s*]:[anti-*p*] = 0.35 (±0.01). Enthalpy values, $\Delta H_{21}°$ = 1.9 (±0.2) kcal mol^{-1} and $\Delta H_{31}°$ = 0.7 (±0.2) kcal mol^{-1},

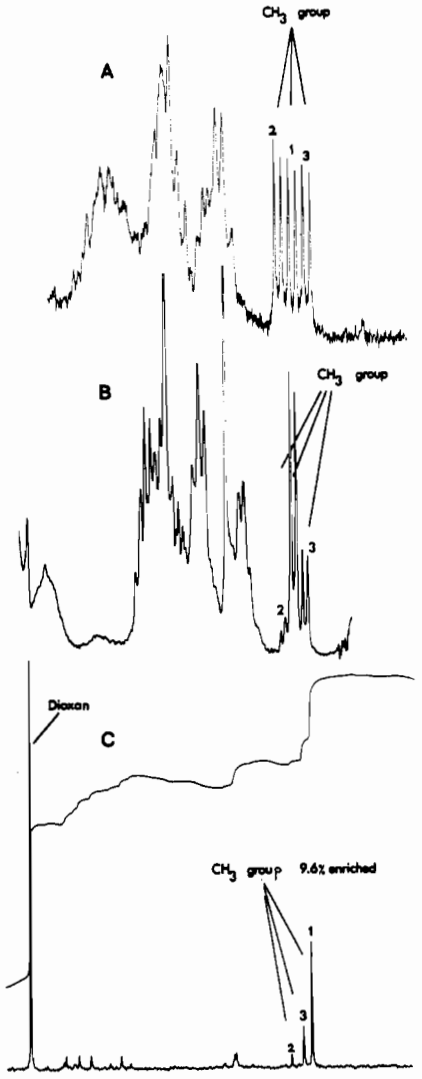

Figure 5. NMR spectra for the three "red" $[Co(Me(tren))(NH_3)Cl]Cl_2$ isomers, anti-*p* (1), syn-*p* (2), and *s* (3): (A) 100-MHz ^1H NMR for a nonequilibrium distribution; (B) 100-MHz ^1H NMR for an equilibrium distribution (~25 °C); (C) ^{13}C NMR for the equilibrium distribution (25 °C).

Table II. Equilibrium Data for Red $[Co(Me(tren))(NH_3)Cl]^{2+}$ Isomers (HCl Solutions, [Co] = 0.1 mol dm^{-3})[a]

80 *T*, °C	[HCl], mol dm^{-3}	K_{21}[e]	K_{31}[e]
80[b]	2	0.204	0.398
80	1	0.205	0.425
80	1	0.214	0.412
40[c]	1	0.137	0.374
40	1	0.135	0.351
25[d]	1	0.126	0.342
25	1	0.127	0.356

[a] $\Delta G° = -RT \ln K$; $\Delta G_{21}° = 1.23 \pm 0.01$ kcal mol^{-1}, $\Delta G_{31}° = 0.63 \pm 0.01$ kcal mol^{-1}. [b] Equilibrium complete in 2 h. [c] Equilibrium complete in 20 h. [d] Equilibrium complete in 2 weeks. [e] See text.

were obtained from plots of log *K* vs. T^{-1}. The larger temperature dependence of the syn-*p*:anti-*p* ratio was used to advantage in preparing larger quantities of the syn-*p* isomer at higher temperatures (cf. Experimental Section). Also, the $\Delta H°$ values have a bearing on the energy minimization calculations, and a discussion of these will be returned to later.

The 100-MHz ^1H NMR spectra for the three isolated chloro isomers in 0.1 mol dm^{-3} DCl and Me_2SO-d_6 are given in Figure 6. They show resemblances to those for *p*-$[Co(tren)(NH_3)Cl]^{2+}$ in the same solvents.[9] In 0.1 mol dm^{-3} DCl each

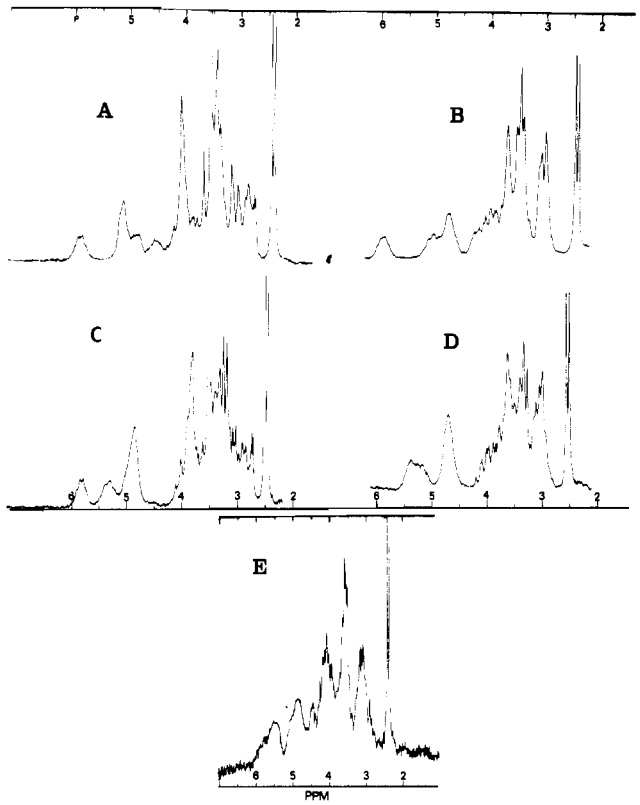

Figure 6. ^{1}H NMR spectra (100 MHz) for the three "red" [Co(Me(tren))(NH_3)Cl]Cl_2 isomers: (A) anti-*p* in Me_2SO-d_6; (B) anti-*p* in 0.1 mol dm^{-3} DCl; (C) syn-*p* in Me_2SO-d_6; (D) syn-*p* in 0.1 mol dm^{-3} DCl; (E) *s* in 0.1 mol dm^{-3} DCl. All are referenced to Me_4Si or NaTPS.

shows partly resolved broad resonances at low field due to the five NH protons. For the anti-*p* isomer these are at δ 5.9 (1 H), 5.0 (1 H), 4.7 (2 H), and 4.2 (1 H) with the last being partly obscured by the methylene protons. For the syn-*p* isomer they are at 5.4 (1 H), 5.2 (1 H), and 4.7 (3 H) ppm and for the *s* isomer at 5.6 (1 H), 5.3 (2 H), and 4.7 (1 H) ppm relative to Me_4Si. Spin-decoupling experiments showed that in each case the NH resonance at lowest field is coupled to the CH_3 group and hence can be assigned to the *sec*-NH proton. The broad resonances in the region of 4.0, 3.7, and 4.0 ppm, respectively, are sharpened and moved to higher fields on addition of D_2SO_4 and are assigned to the NH_3 protons. The CH_3 doublets occur at 2.42, 2.52, and 2.30 ppm for the anti-*p*, syn-*p*, and *s* isomers, respectively (J = 6 Hz). In Me_2SO-d_6 the NH and NH_3 resonances are sharpened somewhat and show substantial chemical shift differences compared to the those of the aqueous spectra, suggesting that H-bonding or other solvent effects play an important role in determining the chemical shift positions.

Proton exchange was examined in part for the anti-*p* and syn-*p* isomers by monitoring the collapse of the N–H signals and the CH_3 doublet in DOAc buffers. For the syn-*p* isomer the two protons at lowest field (5.4, 5.2 ppm) gave linear plots of log [(peak height)$_t$ − (peak height)$_\infty$] vs. time (~3 half-lives), and data are given in Table III. The NH_3 signal at 3.7 ppm also lost intensity at a similar rate and, as expected, so too did the CH_3 doublet collapse to a singlet. The results are consistent with the rate expression

$$-\mathrm{d[H\text{–}complex]}/\mathrm{d}t = k_{ex}[\mathrm{H\text{–}complex}][OD^-]$$

with k_{ex} = 2.5 (±0.5) × 10^5 mol^{-1} dm^3 s^{-1}. When k_{ex} is compared with k_{OH} for base hydrolysis of chloride (Table VII), it is obvious that H exchange is some 10^2 times faster. Such a large difference does not occur however for the two NH

Table III. Rate Data for H Exchange for *syn-p*-[Co(Me(tren))(NH_3)Cl]$^{2+}$ at 25 °C[a]

pD[b]	[DOAc], mol dm^{-3}	[Co], mol dm^{-3}	$10^5 k_{obsd}$,[c] s^{-1} (5.4 and 5.2 ppm)	$10^{-5} k_{ex}$,[d] mol^{-1} dm^3 s^{-1}
4.84	0.1	0.2	5.8 (2)	2.7
4.93	0.1	0.1	7.7 (2)	2.9
5.12	0.05	0.2	8.8 (2)	2.1
5.16	0.1	0.2	9.0 (2)	2.0
5.56	0.1	0.2	23 (2)	2.0

[a] Ionic strength variable (≃1). [b] pD = pH + 0.4.[12] [c] Values in parentheses give number of protons involved. [d] K_{D_2O} = 14.50 (25 °C, I = 1.0 mol dm^{-3}) from extrapolation of data in ref 23; $k_{ex} = k_{obsd}/[OD^-]$.

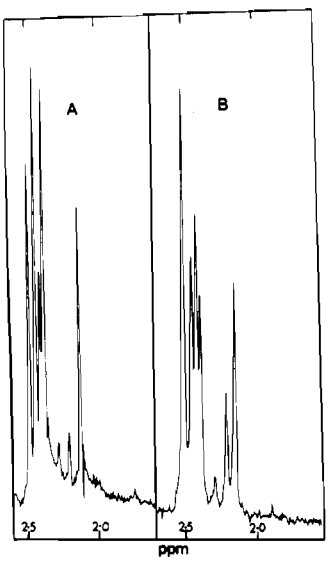

Figure 7. ^{1}H NMR spectra (100 MHz) showing H exchange and aquation in the *anti-p*-[Co(Me(tren))(NH_3)Cl]$^{2+}$ ion, 0.2 mol dm^{-3} DOAc buffer (pH 4.32): (A) after 10 min; (B) after 30 min. The methyl signals from high to low field are DOAc-OAc (2.15 ppm), *s*-aqua (2.21), *s*-chloro (2.29, impurity), anti-*p*-chloro (centered at 2.42), and anti-*p*-aqua (2.51).

protons at lowest field in the anti-*p* isomer. That at 5.9 ppm (coupled to CH_3) and that at 5.0 ppm do not exchange appreciably prior to base hydrolysis of chloride. This is demonstrated for the former proton by Figure 7, where both H exchange and base hydrolysis is accompanied by collapse of the associated CH_3 doublet at 2.42 ppm. Some H exchange in the chloro complex occurs as seen by the appearance of the singlet at the midpoint of the chloro doublet, but experiments at varying [DOAc] showed that this process is largely OAc^- catalyzed (a small OD^--independent path is also involved). However, base hydrolysis is not OAc^- catalyzed. The latter process gives the two singlets at lower (2.51 ppm) and higher (2.21 ppm) fields corresponding to the anti-*p*-aqua and *s*-aqua products. It will be shown later that the *s*-aqua isomer results from the anti-*p*-aqua product in a subsequent process. In other experiments using lower DOAc concentrations, or MES buffers, H exchange was reduced or eliminated entirely without affecting to any great extent the base hydrolysis process. Thus H exchange is not a part of base hydrolysis for the NH proton at lowest field (5.9 ppm), provided of course that every act of OD^--induced exchange does not result in loss of chloride. However, these H-exchange experiments showed that the NH protons at 4.7 ppm (2 H) and at 4.2 ppm (1 H), as well as the NH_3 protons at 4.0 ppm, exchanged rapidly at pH >3 so that any one of these could be responsible for base hydrolysis.

The ^{13}C spectra for the anti-*p* and syn-*p* isomers are given in Table IV, and tentative assignments are made on the basis of the spectrum of the unsubstituted *p*-[Co(tren)(NH_3)Cl]$^{2+}$

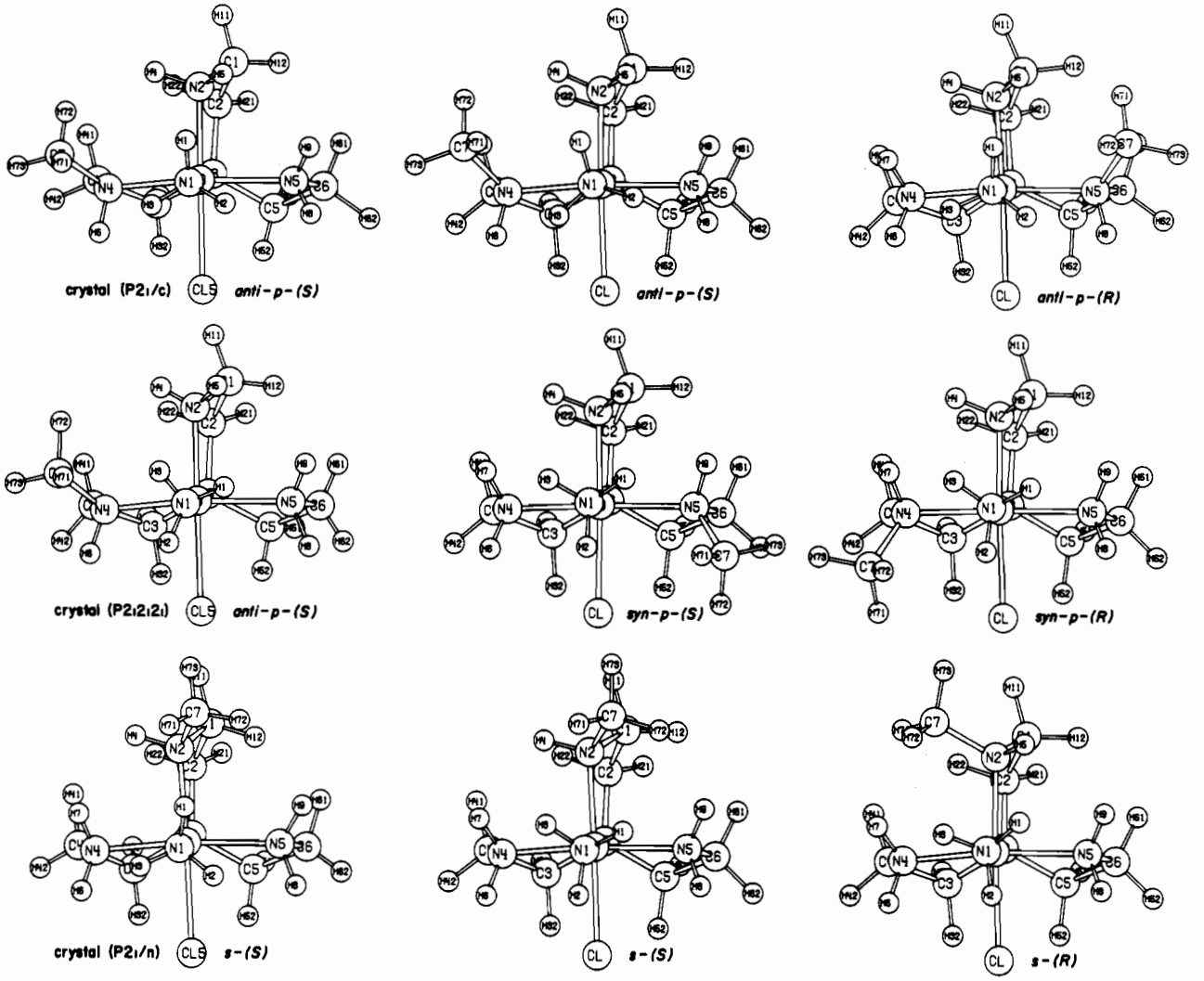

Figure 8. Crystal and minimized structures for the $[Co(Me(tren))(NH_3)Cl]^{2+}$ molecular ions. First column: crystal ($P2_1/c$), racemate anti-*p*-(*RS*); crystal ($P2_12_12_1$), optically active $(+)_{505}$-anti-*p*-(*S*); crystal ($P2_1/n$), racemate *s*-(*RS*). The structures of minimum energy are depicted in the other two columns.

ion. The latter shows four C signals with an intensity ratio 2:1:2:1, and these are assigned as in structure a below. In-

troduction of the methyl group introduces asymmetry, and all seven C signals are now distinguished (in the syn-*p* ion). In comparison to the situation in the unsubstituted molecule one C is shifted to lower field in both isomers, and this is tentatively assigned to C_3 (structures b and c).

3. Crystal[24] and Strain-Energy-Minimized Structures. The geometries of the three "red" $[Co(Me(tren))(NH_3)Cl]^{2+}$ isomers related to that of the *p*-$[Co(tren)(NH_3)Cl]^{2+}$ ion[9] were established by crystal structures on two of them: the racemic and optically active forms of the anti-*p* isomer and the racemic *s* isomer. Figure 8 depicts the crystal cations, and Figure 9 gives details of H bonding to the associated $ZnCl_4^{2-}$ cations. Tables V and VI contain the final atom coordinates and details of the cation geometries, respectively, with use of the same orthogonal coordinate system as that used for the energy-minimized structures (see below).

The crystal geometries of the racemic and optically active anti-*p* cations agree within experimental error (Table VI) except for the Co–Cl bond lengths. In the racemic crystal ($P2_1/c$) Cl(5) is involved in intermolecular H bonding with

Table IV. ^{13}C Absorptions for *p*-$[Co(tren)(NH_3)Cl]^{2+}$ and Some of the $[Co(Me(tren))(NH_3)Cl]^{2+}$ Isomers

	peak assignt[a]	rel intens	δ[b]
(a) *p*-$[Co(tren)(NH_3)Cl]^{2+}$	1	2	4.16
	2	1	6.23
	3	2	20.78
	4	1	21.30
(b) *anti-p*-$[Co(Me(tren))(NH_3)Cl]^{2+}$	1	1	3.63
	1′	1	4.93
	2	1	6.23
	3	1	9.35
	3′, 4	2	21.04
	5	1	29.61
(c) *syn-p*-$[Co(Me(tren))(NH_3)Cl]^{2+}$	1	1	3.93
	1′	1	4.67
	2	1	6.33
	3	1	9.90
	3′	1	21.62
	4	1	23.02
	5	1	27.17

[a] Cf. text. [b] Shift from dioxane (reference).

(24) Crystal positional coordinates and thermal parameters, together with lists of F_o and F_c, in the supplementary material.

Table V. Final Positional Angstrom Orthogonal Coordinates of the Crystal and Minimized Structures of the Isomers of λλδ-$[Co(Me(tren))NH_3Cl]^{2+}$

		anti-*p*-(S)			anti-*p*-(R)	syn-*p*-(S)	syn-*p*-(R)	*s*-(S)		*s*-(R)	
		crystal ($P2_1/a$)	crystal ($P2_12_12_1$)	minimized	minimized	minimized	minimized	crystal ($P2_1/n$)	minimized	minimized	
Co	*x*	0.000(1)	0.000(1)	0.000	0.000	0.000	0.000	0.000(2)	0.000	0.000	
	y	0.000(1)	0.000(1)	0.000	0.000	0.000	0.000	0.000(2)	0.000	0.000	
	z	0.000(1)	0.000(1)	0.000	0.000	0.000	0.000	0.000(1)	0.000	0.000	
N(1)	*x*	1.979(5)	1.974(6)	1.947	1.948	1.947	1.946	1.955(9)	1.948	1.948	
	y	0.000(5)	0.000(6)	0.000	0.000	0.000	0.000	0.000(9)	0.000	0.000	
	z	0.000(5)	0.000(6)	0.000	0.000	0.000	0.000	0.000(9)	0.000	0.000	
N(2)	*x*	−0.050(5)	−0.053(5)	−0.006	−0.022	0.054	0.047	−0.109(8)	−0.064	0.020	
	y	1.942(5)	1.938(5)	1.953	1.955	1.951	1.953	1.952(8)	1.977	1.977	
	z	0.000(5)	0.000(5)	0.000	0.000	0.000	0.000	0.000(8)	0.000	0.000	
N(3)	*x*	−1.961(4)	−1.959(5)	−1.937	−1.939	−1.932	−1.931	−1.949(8)	−1.943	−1.935	
	y	0.070(4)	0.088(5)	0.078	0.078	0.149	0.142	0.035(8)	0.053	0.094	
	z	−0.030(4)	0.000(5)	−0.032	0.036	0.031	−0.045	0.038(8)	−0.010	−0.016	
N(4)	*x*	−0.140(5)	−0.105(5)	−0.104	−0.051	−0.046	−0.105	−0.087(7)	−0.060	−0.087	
	y	−0.160(5)	−0.142(5)	−0.178	−0.056	−0.041	−0.063	−0.038(7)	−0.051	−0.201	
	z	1.969(5)	1.967(5)	1.971	1.956	1.955	1.978	1.932(7)	1.951	1.946	
N(5)	*x*	−0.134(5)	−0.134(5)	−0.076	−0.117	−0.133	−0.067	−0.150(8)	−0.105	−0.078	
	y	−0.052(5)	−0.078(5)	−0.022	−0.158	−0.068	−0.037	−0.178(8)	−0.144	−0.024	
	z	−1.967(5)	−1.967(5)	−1.956	−1.969	−1.977	−1.953	−1.939(8)	−1.947	−1.953	
Cl	*x*	0.105(3)	0.098(2)	0.064	0.067	−0.009	−0.001	0.114(3)	0.062	0.031	
	y	−2.298(2)	−2.285(2)	−2.233	−2.236	−2.236	−2.237	−2.287(3)	−2.238	−2.236	
	z	−0.035(2)	−0.032(2)	−0.108	0.072	0.078	−0.087	0.057(3)	0.053	−0.105	
C(1)	*x*	−1.337(6)	−1.328(6)	−1.318	−1.359	−1.246	−1.234	−1.412(10)	−1.352	−1.307	
	y	2.414(6)	2.432(6)	2.415	2.430	−2.456	2.446	2.360(10)	2.359	2.428	
	z	−0.582(6)	−0.584(6)	−0.538	−0.462	−0.530	−0.566	−0.573(10)	−0.650	−0.525	
C(2)	*x*	−2.426(6)	−2.420(6)	−2.400	−2.429	−2.354	−2.356	−2.446(11)	−2.437	−2.382	
	y	1.520(6)	1.543(6)	1.513	1.508	1.596	1.588	1.439(11)	1.474	1.532	
	z	−0.088(6)	−0.039(6)	−0.012	0.068	0.011	−0.074	−0.041(11)	−0.104	0.023	
C(3)	*x*	−2.435(6)	−2.421(6)	−2.392	−2.349	−2.369	−2.399	−2.376(10)	−2.364	−2.390	
	y	−0.555(6)	−0.570(6)	−0.638	−0.624	−0.505	−0.521	−0.603(10)	−0.565	−0.630	
	z	1.229(6)	1.245(6)	1.205	1.296	1.308	1.216	1.346(10)	1.291	1.217	
C(4)	*x*	−1.576(6)	−1.540(6)	−1.551	−1.472	−1.470	−1.556	−1.518(11)	−1.491	−1.522	
	y	−0.028(6)	−0.078(6)	−0.173	−0.133	−0.025	−0.024	0.015(11)	−0.007	−0.206	
	z	2.362(6)	2.389(6)	2.367	2.422	2.420	2.363	2.386(11)	2.388	2.375	
C(5)	*x*	−2.390(6)	−2.446(6)	−2.369	−2.401	−2.413	−2.375	−2.392(10)	−2.376	−2.380	
	y	−0.672(6)	−0.643(6)	−0.625	−0.638	−0.587	−0.588	−0.791(10)	−0.755	−0.596	
	z	−1.256(6)	−1.230(6)	−1.285	−1.199	−1.184	−1.279	−1.158(10)	−1.198	−1.273	
C(6)	*x*	−1.564(6)	−1.589(6)	−1.494	−1.566	−1.584	−1.485	−1.587(11)	−1.525	−1.499	
	y	−0.205(6)	−0.204(6)	−0.171	−0.177	−0.161	−0.183	−0.360(11)	−0.367	−0.162	
	z	−2.420(6)	−2.404(7)	−2.425	−2.366	−2.368	−2.426	−2.379(11)	−2.381	−2.417	
C(7)	*x*	0.736(6)	0.729(7)	0.672	0.656	0.667	0.596	0.979(11)	1.070	0.355	
	y	0.580(6)	0.663(7)	0.777	0.817	−1.120	−1.187	2.742(11)	2.739	2.695	
	z	2.879(6)	2.833(7)	2.829	−2.807	−2.690	2.682	−0.474(11)	−0.620	1.272	
H(1)	*x*	2.287	2.109	2.318	2.325	2.295	2.286	2.319	2.300	2.292	
	y	0.892	0.321	0.900	0.916	0.473	0.405	0.871	0.349	0.597	
	z	0.016	−0.832	0.225	−0.129	−0.809	−0.849	−0.207	−0.868	−0.724	
H(2)	*x*	2.294	2.548	2.292	2.288	2.323	2.325	2.302	2.316	2.318	
	y	−0.446	−0.785	−0.264	−0.592	−0.926	−0.921	−0.605	−0.919	−0.915	
	z	−0.790	0.309	−0.900	−0.730	0.017	0.078	−0.695	0.133	−0.152	
H(3)	*x*	2.283	2.148	2.286	2.286	2.275	2.279	2.319	2.286	2.289	
	y	−0.462	0.684	−0.658	−0.355	0.486	0.549	−0.298	0.572	0.334	
	z	0.763	0.515	0.672	0.871	0.810	0.767	0.819	0.746	0.878	
H(4)	*x*	0.065	−0.080	0.133	0.143	0.195	0.152	−0.066	−0.117		
	y	2.262	2.371	2.349	2.305	2.316	2.331	2.295	2.265		
	z	0.927	0.718	0.903	0.921	0.920	0.919	0.893	0.957		
H(5)	*x*	0.635	0.670	0.723	0.687	0.798	0.811			0.715	
	y	2.217	2.395	2.292	2.333	2.283	2.281			2.243	
	z	−0.580	−0.558	−0.595	−0.594	−0.580	−0.556			−0.668	
H(6)	*x*	0.151	−0.012	0.261	0.447	0.405		0.339	0.369	0.329	
	y	−1.075	−1.034	−1.088	−0.856	−0.868		−0.825	−0.888	−1.074	
	z	2.135	2.289	2.173	2.290	2.289		2.246	2.291	2.198	
H(7)	*x*				0.390	0.440	0.325	0.167	0.439	0.412	
	y				0.750	0.739	0.778	0.773	0.720	0.501	
	z				2.350	2.347	2.305	2.194	2.348	2.448	
H(8)	*x*	0.412	0.290	0.469	0.263		0.480	0.312	0.460	0.464	
	y	−0.725	−0.995	−0.782	−1.058		−0.804	−1.039	−0.914	−0.792	
	z	−2.378	−2.376	−2.310	−2.183		−2.290	−2.244	−2.244	−2.298	
H(9)	*x*	0.388	0.121	0.314		0.221	0.329	0.093	0.252	0.318	
	y	0.672	0.713	0.821		0.814	0.800	0.600	0.674	0.811	
	z	−2.364	−2.324	−2.326		−2.290	−2.331	−2.494	−2.393	−2.334	
H(11)	*x*	−1.539	−1.407	−1.509	−1.536	−1.396	−1.401	−1.689	−1.589	−1.509	
	y	3.383	3.403	3.437	3.436	3.486	3.480	3.345	3.398	3.456	
	z	−0.323	−0.265	−0.202	−0.074	−0.199	−0.276	−0.391	−0.415	−0.217	
H(12)	*x*	−1.266	−1.213	−1.309	−1.408	−1.245	−1.193	−1.137	−1.283	−1.311	
	y	2.386	2.314	2.422	2.490	2.458	2.429	2.026	2.268	2.414	
	z	−1.549	−1.533	−1.626	−1.546	−1.619	−1.674	−1.508	−1.732	−1.613	
H(21)	*x*	−3.346	−3.336	−3.293	−3.320	−3.240	−3.224	−3.298	−3.308	−3.289	
	y	1.546	1.704	1.636	1.620	1.728	1.720	1.626	1.537	1.665	
	z	−0.620	−0.668	−0.625	−0.536	−0.611	−0.722	−0.611	−0.758	−0.568	
H(22)	*x*	−2.604	−2.638	−2.658	−2.675	−2.609	−2.642	−2.646	−2.740	−2.614	
	y	1.912	1.799	1.835	1.822	1.950	1.942	1.735	1.856	1.849	
	z	0.867	0.889	0.996	1.079	1.010	0.915	0.732	0.870	1.039	
H(31)	*x*	−3.472	−3.557	−3.443	−3.394	−3.404	−3.448	−3.248	−3.410	−3.432	
	y	−0.415	−0.400	−0.418	−0.407	−0.238	−0.280	−0.202	−0.331	−0.387	
	z	1.290	1.485	1.398	1.522	1.529	1.397	1.402	1.496	1.428	
H(32)	*x*	−2.336	−2.338	−2.289	−2.249	−2.312	−2.310	−2.215	−2.261	−2.317	
	y	−1.441	−1.564	−1.717	−1.705	−1.590	−1.605	−1.554	−1.649	−1.710	
	z	1.143	1.088	1.094	1.199	1.236	1.146	1.294	1.264	1.089	
H(41)	*x*	−1.660	−1.749	−1.863	−1.805	−1.749	−1.839	−1.727	−1.778	−1.816	
	y	0.940	0.780	0.822	0.845	0.982	0.993	1.078	1.018	0.781	
	z	2.579	2.593	2.683	2.771	2.732	2.633	2.433	2.623	2.734	
H(42)	*x*	−1.756	−1.815	−1.701	−1.546	−1.582	−1.741	−1.676	−1.618	−1.655	
	y	−0.419	−0.806	−0.851	−0.828	−0.686	−0.653	−0.398	−0.609	−0.912	
	z	3.313	3.104	3.209	3.261	3.282	3.236	3.238	3.290	3.197	
H(51)	*x*	−3.250	−3.590	−3.412	−3.454	−3.465	−3.412	−3.351	−3.426	−3.418	
	y	−0.418	−0.707	−0.397	−0.428	−0.364	−0.340	−0.701	−0.566	−0.346	
	z	−1.480	−1.605	−1.509	−1.391	−1.370	−1.513	−1.330	−1.422	−1.495	
H(52)	*x*	−2.250	−2.298	−2.289	−2.295	−2.324	−2.324	−2.245	−2.274	−2.324	
	y	−1.555	−1.539	−1.706	−1.717	−1.664	−1.667	−1.745	−1.823	−1.679	
	z	−1.038	−1.056	−1.177	−1.086	−1.051	−1.139	−0.984	−1.009	−1.167	
H(61)	*x*	−1.791	−1.757	−1.871	−1.903	−1.945	−1.845	−1.817	−1.931	−1.866	
	y	0.692	0.638	0.766	0.802	0.795	0.747	0.580	0.529	0.775	
	z	−2.770	−2.781	−2.836	−2.700	−2.747	−2.866	−2.722	−2.852	−2.836	
H(62)	*x*	−1.709	−1.608	−1.536	−1.704	−1.721	−1.532	−1.675	−1.557	−1.550	
	y	−0.896	−0.960	−0.917	−0.872	−0.890	−0.953	−0.935	−1.171	−0.914	
	z	−3.361	−2.868	−3.222	−3.196	−3.168	−3.199	−3.055	−3.119	−3.207	
H(71)	*x*	1.633	1.547	1.690	0.262	1.697	0.059	1.782	1.973	−0.415	
	y	0.442	0.603	0.887	1.826	−1.129	−2.125	2.564	2.632	2.528	
	z	2.729	2.635	2.459	−2.714	−2.338	2.543	0.018	−0.020	2.023	
H(72)	*x*	0.549	0.557	0.195	1.705	0.230	1.613	1.173	1.270	1.320	
	y	1.473	1.733	1.755	0.820	−2.106	−1.297	2.534	2.394	2.359	
	z	2.763	2.783	2.866	−2.516	−2.539	2.308	−1.406	−1.633	1.651	
H(73)	*x*	0.455	0.413	0.710	0.588	0.667	0.637	0.794	0.827	0.420	
	y	0.343	0.476	0.397	0.528	−0.916	−0.982	3.672	3.802	3.768	
	z	3.805	3.793	3.851	−3.857	−3.762	3.753	−0.435	−0.655	1.085	

Table VI. Comparison of Crystal and Minimized Structures of λλδ-[Co(Metren)NH$_3$Cl]$^{2+}$

(i) Bond lengths (Å)

	anti-p-(S)			*anti-p-(R)*	*syn-p-(S)*	*syn-p-(R)*	*s-(S)*		*s-(R)*
	crystal ($P2_1/c$)	crystal ($P2_12_12_1$)	mini-mised	minimised	minimised	minimised	crystal ($P2_1/n$)	mini-mised	mini-mised
Co-Cl	2.301(2)	2.288(2)	2.237	2.238	2.238	2.238	2.291(4)	2.239	2.239
Co-N(1)	1.979(5)	1.974(5)	1.948	1.948	1.947	1.946	1.955(9)	1.948	1.948
N(2)	1.943(5)	1.939(5)	1.953	1.955	1.952	1.954	1.955(10)	1.978[a]	1.977[a]
N(3)	1.962(4)	1.961(5)	1.939	1.941	1.938	1.937	1.950(8)	1.944	1.937
N(4)	1.981(5)	1.975(6)	1.981[a]	1.957	1.956	1.981[a]	1.935(9)	1.953	1.959
N(5)	1.972(5)	1.974(6)	1.958	1.979[a]	1.983[a]	1.955	1.953(8)	1.955	1.955
N(3)-C(2)	1.523(7)	1.526(8)	1.508	1.508	1.508	1.508	1.491(14)	1.508	1.507
C(3)	1.484(7)	1.482(8)	1.500	1.500	1.500	1.499	1.517(13)	1.500	1.501
C(5)	1.496(6)	1.511(8)	1.500	1.501	1.499	1.500	1.520(12)	1.500	1.501
N(2)-C(1)	1.490(7)	1.487(8)	1.492	1.493	1.492	1.492	1.481(14)	1.493	1.496
N(4)-C(4)	1.495(8)	1.497(8)	1.500	1.498	1.498	1.502	1.502(13)	1.497	1.498
N(5)-C(6)	1.507(7)	1.524(8)	1.501	1.502	1.506	1.502	1.514(13)	1.502	1.501
C(1)-C(2)	1.493(8)	1.510(10)	1.503	1.502	1.503	1.503	1.484(16)	1.502	1.503
C(3)-C(4)	1.517(8)	1.525(9)	1.508	1.509	1.508	1.509	1.483(15)	1.509	1.508
C(5)-C(6)	1.502(8)	1.519(9)	1.507	1.507	1.507	1.506	1.525(15)	1.508	1.508
N(2)-C(7)							1.426(13)	1.500	1.499
N(4)-C(7)	1.464(7)	1.448(8)	1.500			1.501			
N(5)-C(7)				1.500	1.501				
Zn-Cl(1)	2.254(2)	2.240(2)					2.274(3)		
Cl(2)	2.296(2)	2.266(2)					2.278(3)		
Cl(3)	2.247(2)	2.265(2)					2.265(3)		
Cl(4)	2.278(2)	2.329(2)					2.256(3)		

(ii) Bond Angles (°)

Cl-Co-N(1)	87.4(1)	87.5(2)	88.4	88.3	90.2	90.0	87.1(3)	88.4	89.2
N(2)	178.6(1)	178.8(2)					178.5(3)		
N(3)	94.7(1)	95.0(2)	93.9	94.0	94.1	94.1	93.9(3)	93.1	93.5
N(4)	86.4(1)	86.8(2)	87.7	86.6	86.8	90.4	87.6(3)	87.2	86.9
N(5)	87.8(1)	87.0(2)	86.7	87.4	90.0	86.7	86.4(3)	87.2	86.6
N(1)-Co-N(2)	91.5(2)	91.6(2)	90.2	90.6	88.4	88.6	93.2(4)	91.8	89.4
N(3)	177.8(2)	177.4(2)					178.5(4)		
N(4)	94.1(2)	93.0(2)	93.0	91.5	91.4	93.0	92.6(4)	91.7	92.6
N(5)	93.9(2)	93.9(2)	92.2	93.4	93.8	92.0	94.4(4)	93.1	92.3
N(2)-Co-N(3)	86.5(2)	85.9(2)	87.5	87.0	87.2	87.2	85.8(4)	86.6	87.8
N(4)	94.5(2)	94.0(2)	95.1	91.6	91.2	91.9	91.0(4)	91.4	95.9[a]
N(5)	91.4(2)	92.2(2)	90.6	94.5	92.1	91.1	95.0(4)	94.1	90.7
N(3)-Co-N(4)	87.0(2)	87.1(2)	88.1	87.5	87.8	88.4	86.3(4)	88.6	88.2
N(5)	85.3(2)	86.2(2)	86.8	87.9	87.2	86.8	86.8(4)	86.7	87.3
N(4)-Co-N(5)	169.9(2)	170.5(2)					170.6(4)		
Co-N(3)-C(2)	109.8(3)	110.2(4)	110.2	110.9	110.6	110.6	110.5(7)	110.7	110.0
C(3)	106.9(3)	106.9(4)	105.6	105.6	105.7	105.0	106.9(6)	105.4	105.8
C(5)	106.4(3)	107.5(4)	106.4	105.8	105.6	106.2	105.4(6)	106.1	106.3
C(2)-N(3)-C(3)	109.6(4)	110.5(5)	110.5	109.8	110.3	110.6	110.4(9)	110.5	110.4
C(5)	110.7(4)	110.1(5)	111.7	111.9	111.8	111.5	111.9(9)	111.3	111.9
C(3)-N(3)-C(5)	113.2(4)	111.6(5)	112.2	112.6	112.5	112.6	111.6(9)	112.6	112.1
Co-N(2)-C(1)	109.8(3)	110.8(4)	108.2	109.2	108.3	108.1	108.9(7)	106.4	107.0
Co-N(4)-C(4)	108.8(3)	109.2(4)	108.2	109.7	109.4	107.9	110.1(6)	108.7	109.1
Co-N(5)-C(6)	111.5(3)	110.7(4)	110.5	108.7	109.0	110.4	111.9(7)	110.5	110.3
N(3)-C(2)-C(1)	111.1(4)	110.6(5)	110.2	110.5	110.3	110.1	111.8(10)	110.0	110.3
N(3)-C(3)-C(4)	107.9(4)	107.9(5)	108.6	108.4	108.4	108.6	105.5(10)	108.4	108.7
N(3)-C(5)-C(6)	108.8(5)	107.9(5)	108.9	108.7	108.8	108.7	108.8(9)	108.7	109.2
N(2)-C(1)-C(2)	108.1(5)	106.4(5)	108.7	109.1	108.7	108.6	107.7(10)	108.3	109.1
N(4)-C(4)-C(3)	108.5(4)	109.2(5)	109.5	109.6	109.5	109.7	108.9(10)	109.3	109.4
N(5)-C(6)-C(5)	108.7(5)	110.0(5)	110.0	109.5	110.1	110.1	107.6(9)	110.2	110.2
Co-N(2)-C(7)							120.7(8)	118.9[a]	118.8[a]
Co-N(4)-C(7)	122.3(4)	121.7(4)	119.0[a]			117.9[a]			
Co-N(5)-C(7)				118.3[a]	117.5[a]				
C(1)-N(2)-C(7)							113.0(10)	110.0	110.6
C(4)-N(4)-C(7)	111.5(4)	111.1(5)	110.3			110.5			
C(6)-N(5)-C(7)				111.0	110.3				
Cl(1)-Zn-Cl(2)	109.73(7)	114.00(7)					113.06(13)		
Cl(3)	110.63(7)	109.68(7)					107.83(12)		
Cl(4)	109.36(7)	108.75(8)					112.20(12)		
Cl(2)-Zn-Cl(3)	109.26(6)	110.45(7)					111.72(12)		
Cl(4)	106.14(6)	103.41(7)					104.74(12)		
Cl(3)-Zn-Cl(4)	111.61(6)	110.36(8)					107.17(13)		

[a] Strain energy >0.4 kcal mol^{-1}

(iii) Intramolecular Non-bonded Interactions (>0.4 kcal mol^{-1})

	anti-p-(S)				*anti-p-(R)*		*syn-p-(S)*		*syn-p-(R)*		*s-(S)*			*s-(R)*	
	crystal ($P2_1/c$)	crystal ($P2_12_12_1$)	mini-mised	strain energy	mini-mised	strain energy	mini-mised	strain energy	mini-mised	strain energy	crystal ($P2_1/n$)	mini-mised	strain energy	mini-mised	strain energy
Cl-C(7)							3.061	0.50	3.021	0.61					
N(2)							2.676	0.41	2.677	0.41	2.86	2.613	0.61	2.642	0.51
N(6)	2.49	2.64	2.560	0.83	2.640	0.52	2.633	0.54			2.64	2.631	0.55	2.597	0.67
N(4)	2.84	2.68	2.668	0.43	2.551	0.87			2.672	0.42	2.63	2.682	0.40	2.661	0.46
N(32)	2.84	2.78	2.692	0.37	2.630	0.55	2.658	0.46	2.693	0.37	2.74	2.685	0.39	2.687	0.38
N(52)	2.67	2.71	2.637	0.53	2.681	0.40	2.639	0.52	2.613	0.61	2.63	2.599	0.66	2.642	0.51
N(72)							2.632	0.55							
C(3)-H(22)	2.50	2.41	2.497	0.38	2.477	0.42	2.485	0.41	2.494	0.38	2.43	2.486	0.41	2.495	0.38
C(7)-H(42)									2.461	0.47					
H(62)							2.446	0.52							
N(4)-H(7)					2.125	0.59	2.140	0.55	2.089	0.72	2.02	2.152	0.52		
H(72)	2.06	2.25	2.052	0.87											
N(9)-H(72)											2.47	2.139	0.56		
N(12)-H(61)	2.15	2.16	2.126	0.60	2.103	0.67	2.127	0.59	2.162	0.49	2.01	2.168	0.48	2.119	0.62
N(22)-H(41)	2.18	2.18	2.123	0.61	2.138	0.56	2.155	0.51	2.121	0.61	2.04	2.168	0.48	2.157	0.51

(iv) Torsion Angles (°) (>0.4 kcal mole^{-1})

	anti-p-(S)				*anti-p-(R)*		*syn-p-(S)*	
	crystal ($P2_1/c$)	crystal ($P2_12_12$)	mini-mised	strain energy	mini-mised	strain energy	mini-mised	strain energy
Co-N(2)-C(1)-C(2)	39.9(5)	41.7(6)	+39.1	0.42	+36.9	0.50	+39.6	0.40
Co-N(3)-C(2)-C(1)	20.0(5)	21.6(6)	+23.5	1.03	+22.0	1.08	+21.1	1.12
Co-N(4)-C(4)-C(3)	30.1(5)	26.1(6)	+24.7	0.98	+19.8	1.16	+21.4	1.10
Co-N(5)-C(6)-C(5)	-16.6(5)	-16.8(6)	-15.2	1.31	-23.2	1.04	-17.1	1.25
N(2)-C(1)-C(2)-N(3)	-38.7(6)	-40.3(7)	-41.0	0.57	-38.3	0.72	-39.6	0.65
N(3)-C(3)-C(4)-N(4)	-49.2(5)	-46.6(7)	-46.5	0.30	-43.3	0.45	-44.1	0.41
N(3)-C(5)-C(6)-N(5)	41.5(6)	40.0(7)	+39.1	0.67	+45.4	0.35	+42.1	0.51

	syn-p-(R)		*s-(S)*			*s-(R)*	
	mini-mised	strain energy	crystal ($P2_1/n$)	mini-mised	strain energy	mini-mised	strain energy
Co-N(2)-C(1)-C(2)	+40.3	0.38	41.1(10)	+44.1	0.25	+39.4	0.41
Co-N(3)-C(2)-C(1)	+21.8	1.09	19.1(11)	+20.3	1.14	+24.6	0.99
Co-N(4)-C(4)-C(3)	+23.4	1.03	28.9(11)	+25.8	0.94	+23.4	1.03
Co-N(5)-C(6)-C(5)	-13.6	1.35	-18.0(11)	-14.2	1.34	-14.7	1.32
N(2)-C(1)-C(2)-N(3)	-40.6	0.59	-39.2(12)	-42.5	0.49	-42.3	0.50
N(3)-C(3)-C(4)-N(4)	-46.6	0.30	-48.9(12)	-46.7	0.29	-44.8	0.38
N(3)-C(5)-C(6)-N(5)	+38.5	0.71	42.2(12)	+38.9	0.69	+38.3	0.72

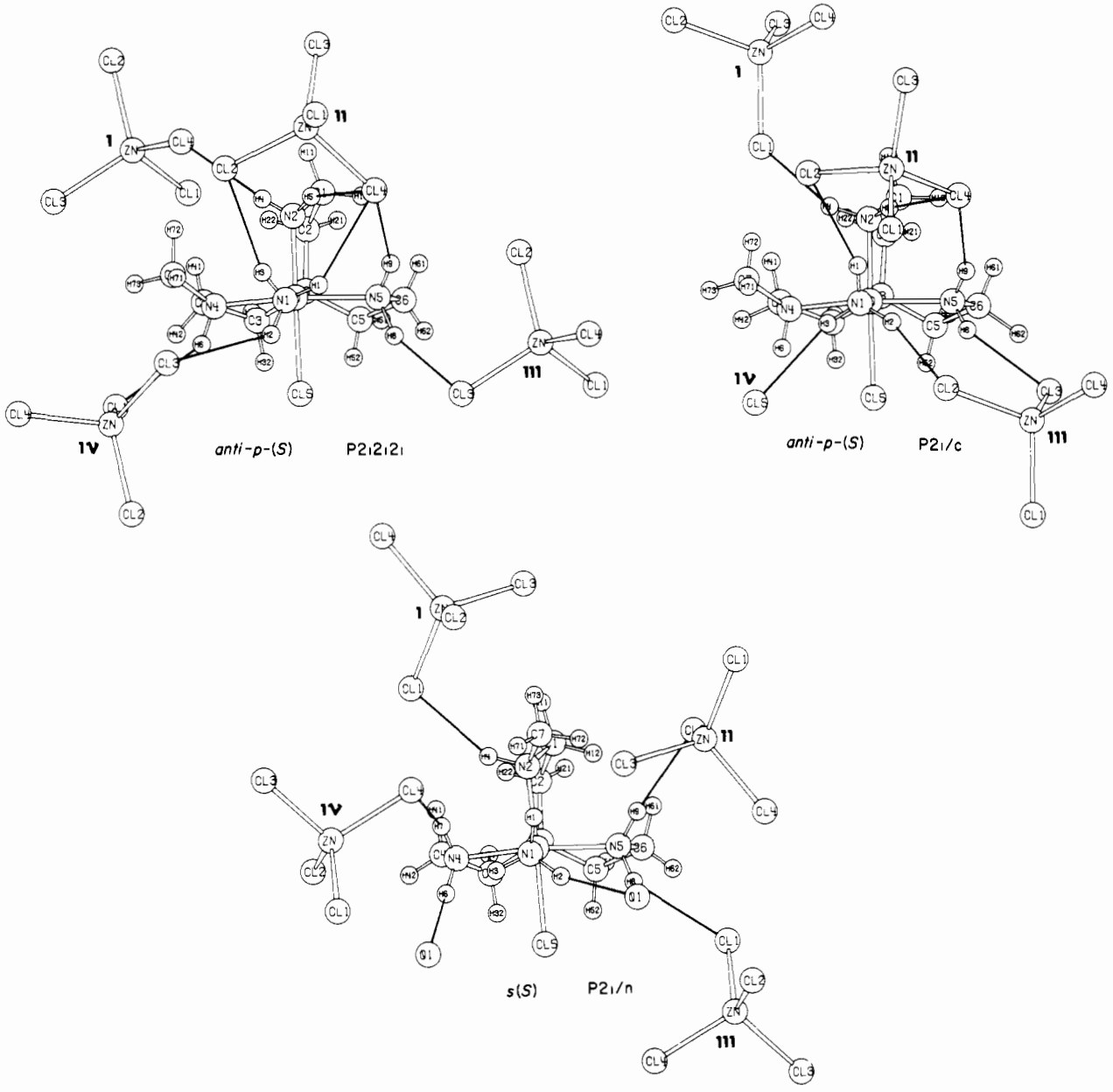

Figure 9. Details of H bonding to the $ZnCl_4^{2-}$ anions and to H_2O in the three crystals (cf. Table XV).

H(3) (Figure 9) whereas in the optically active crystal it is not. This could account for the lengthening from 228.8 (2) to 230.1 (2) pm. Packing of the molecules in the unit cell is most efficient for the *s* isomer (V = 1790.3 (6) Å^3, Table Ia) and least efficient for the optically active anti-*p* ($P2_12_12_1$) crystal (V = 1795.5 (5) Å^3) especially when it is realized that the former contains an additional four water molecules.

Extensive H bonding occurs between the $ZnCl_4^{2-}$ anions and the N–H groups (Figure 9 and Table XV (supplementary material)). The criterion used for a H bond is that $d_{H\text{-}Y} < W_H + W_Y$[19] with use of the van der Waals closest approach distances of Pauling (Cl, 1.8 Å; O, 1.4 Å)[20] and Baur (H, 1.0 Å).[21] In the $P2_12_12_1$ crystal all eight N–H protons are involved. H(2)···Cl(3) and H(9)···Cl(4) are close to the limit of the range and could be considered as being forced on the structure by other H-bonding and packing forces. In the $P2_1/c$ crystal H(6) is not involved although all chlorine atoms of $ZnCl_4^{2-}$ and Cl(5) are, and in the *s* cation H(1) and H(3) are not involved. In the latter crystal the oxygen atoms of the water molecules also act as acceptors (Table XV). The proximity of O(1) to Cl(1), Cl(3), and Cl(5) (332.5 (8), 326.7 (9), and 338.1 (8) pm) infers that the hydrogens of this water molecule (not located) also act as donors. The distributions of the N–H···X bond angles (Table XV) with H···X distance is in agreement with the general criterion[19] that the shorter the latter the more linear the H bond. The considerable constraints placed on the locations of the N–H hydrogen and Zn–Cl chloride atoms by the packing arrangements presumably result in the considerable deviations from the ideal linear behavior observed in other cases.

The relative energies of the three structures have been investigated by the strain energy minimization technique using the program MOL-5 originated by Boyd[25] and subsequently developed by Snow,[26] Maxwell,[27,28] Dwyer[29] and Gainsford.[18,30] The program uses a Newton–Raphson method to minimize the total molecular strain energy considered as the sum of

(25) R. H. Boyd, *J. Chem. Phys.*, **47**, 3736 (1967).
(26) M. R. Snow, *J. Am. Chem. Soc.*, **92**, 3610 (1970).
(27) D. A. Buckingham, I. E. Maxwell, A. M. Sargeson, and M. R. Snow, *J. Am. Chem. Soc.*, **92**, 3617 (1970).
(28) I. E. Maxwell, Ph.D. Thesis, The Australian National University, 1969.
(29) M. Dwyer, Ph.D. Thesis, The Australian National University, 1971.
(30) D. A. Buckingham and A. M. Sargeson, *Top. Stereochem.*, **6**, 219 (1971).

Table VII. Final Strain Energy Terms for the $\lambda\lambda\delta$-$[Co(Me(tren))NH_3Cl]^{2+}$ Cations[31] (kcal mol^{-1})

	anti-*p*-(*S*)	anti-*p*-(*R*)	syn-*p*-(*S*)	syn *p*-(*R*)	*s*-(*S*)	*s*-(*R*)
bond length def	1.28	1.28	1.32	1.29	1.25	1.24
angular def	4.33	4.44	3.72	3.73	4.14	4.36
nonbonded interaction	1.78	1.75	1.90	1.89	1.60	1.60
torsional strain	5.91	5.78	5.98	6.01	5.66	5.89
total strain energy	13.30	13.25	12.92	12.92	12.65	13.09

terms due to bond length deformation, bond angle deformation, nonbonded interactions, and torsional interactions. Details of the energy functions and force fields used are given in ref 9. Initial coordinates for the calculations were obtained from the crystal structures and from the minimized structure of *p*-$[Co(tren)(NH_3)Cl]^{2+}$ ion[9] by including a CH_3 group on the appropriate N center. Six possibilities occur including conformational isomers (but excluding mirror image pairs),[31] and the final minimized structures are depicted in Figure 8. Final strain energy contributions are given in Table VII. It is clear that the structures are related in pairs by the λ or δ possibility for the central apical chelate ring.

The geometry of the minimized structure for the anti-*p* isomer (anti-*p*-(*S*), Figure 8) agrees well with those of the two crystal structures. Significant differences occur only in the shorter Co–Cl bond length (223.7 ppm) and in variations in the Co–N(1), Co–N(3), and N(4)–C(7) bond lengths (Table VI). These differences probably result from an error in the force field constant for Cl and in the fact that the same force constant was used for primary, secondary, and tertiary N. Similar findings and conclusions occur with the crystal and minimized *s* structures (Co–Cl, N(2)–C(7), Table VI).

A comparison of the minimized energy components (Table VII) shows that the *s*-$\lambda\lambda\delta$-(*S*) structure is the most stable and the anti-*p*-$\lambda\lambda\delta$-(*S*) structure the least. However, the complete span of energy differences is only 0.65 kcal mol^{-1}, and differences between the different conformational forms of the same isomer are even less. This predicted stability order *s* > syn-*p* > anti-*p* is not that observed experimentally. As preparations and under equilibrium conditions, the order is anti-*p* > *s* > syn-*p* for each of the chloro, aqua, and hydroxo complexes, and this is independent of counterion. The $\Delta H°$ data (see above) give this same order for the chloro complexes and can be more directly related to the minimized energies, which estimate enthalpy differences. Clearly the energy minimization calculations are not sufficiently refined to account for small energy differences. Thus, whereas the present calculations reproduce the major features of the geometry observed in the crystal[18,26,30] and have in the past predicted the correct stability order for isomers that differ significantly in energy content (>1 kcal mol^{-1}), they are not yet able to cope with experimentally observable equilibrium distributions (i.e., ≤1 kcal mol^{-1}).

4. Aquation, Hg^{2+}-Induced Aquation, and Base Hydrolysis of the "Red" $[Co(Me(tren))(NH_3)Cl]^{2+}$ Isomers. Rate data for the normal aquation and Hg^{2+}-induced aquation reactions are given in Tables VIII and IX, respectively. For both processes the relative order is syn-*p* > *s* > anti-*p* with k_{aq} and $k_{Hg^{2+}}$ having values of $(2.95 \pm 0.1) \times 10^{-5}$ s^{-1} and (1.84 ± 0.04) mol^{-1} dm^3 s^{-1}, $(1.1 \pm 0.1) \times 10^{-5}$ s^{-1} and (0.34 ± 0.03) mol^{-1} dm^3 s^{-1}, and $(1.95 \pm 0.05) \times 10^{-6}$ s^{-1} and $(2.2 \pm 0.2) \times 10^{-2}$ mol^{-1} dm^3 s^{-1}. There is no certain reason for this order although if cleavage of Co–Cl is rate controlling steric crowding in the activated complex might be expected to be greatest with the syn-*p* isomer, which has the CH_3 group adjacent to the leaving group. That this effect is accentuated for the Hg^{2+}-induced reaction, where the leaving group is larger ($HgCl^+$), supports this argument. It is also apparent that the order is the reverse of the stability order for the chloro isomers at equilibrium.

Base hydrolysis follows the expected rate law

$$-d[Co-Cl]/dt = k_{OH}[Co-Cl][OH^-]$$

(31) The chelate ring conformations $\lambda\lambda\delta$ correspond to the three rings from left to right in Figure 8 (i.e., equatorial, apical, equatorial). Those in the same plane are constrained by N_3 to have opposite configurations allowing only the apical ring to be λ or δ. The $\lambda\delta\delta$-anti-*p*-(*S*) and $\lambda\lambda\delta$-anti-*p*-(*R*) forms are then optical enantiomers and must have identical energies.

Table VIII. Kinetic Data[a] for Aquation of "Red" $[Co(Me(tren))(NH_3)Cl]^{2+}$ Isomers at 25.0 °C, μ = 1.0 ($NaClO_4$)

	$[H^+]$, mol dm^{-3}	$10^3[Co]$, mol dm^{-3}	$10^6 k_{obsd}$, s^{-1}
anti-*p*	0.1	9	2.0
	0.1	2.6	2.0
	0.01	2.6	1.85
syn-*p*	1.0	2.1	30.2
	0.01	2.1	28.7
s	1.0	2.0	12.2
	0.01	2.0	10.3

[a] Spectrophotometric data, 550 nm.

Table IX. Kinetic Data for Hg^{2+}-Induced Aquation of "Red" $[Co(Me(tren))(NH_3)Cl]^{2+}$ Isomers at 25.0 °C, μ = 1.0 ($NaClO_4$)

	$[H^+]$, mol dm^{-3}	$[Hg^{2+}]$, mol dm^{-3}	$10^3 \times$ [Co], mol dm^{-3}	$10^3 \times k_{obsd}$, s^{-1}	$10^2 \times k_{calcd}$, mol^{-1} dm^3 s^{-1}
anti-*p*	0.01 (1)[a]	0.1	1.3	2.43	2.4
	0.1 (1)	0.1	1.1	2.08	2.1
	0.1 (1)	0.05	1.1	1.11	2.2
	0.1 (1)	0.01	1.0	0.215	2.1
syn-*p*	0.01 (2)	0.1	0.9	178	178
	0.1 (2)	0.1	0.9	182	182
	0.1 (2)	0.05	0.9	92.9	186
	0.1 (2)	0.01	1.2	18.9	189
s	0.005 (2)	0.05	1.0	14.4	29
	0.05 (1)	0.05	1.0	16.5	33
	0.05 (2)	0.05	0.5	17.4	35
	0.05 (1)	0.025	1.0	7.92	32
	0.05 (1)	0.005	0.5	1.82	36
	0.01 (2)	0.1	0.5	33.8	34
	0.01 (2)	0.1	1.6	39	39

[a] Number of runs in parentheses. [b] $k_{calcd} = k_{obsd}/[Hg^{2+}]$.

Table X. Kinetic Data for Base Hydrolysis of "Red" $[Co(Me(tren))(NH_3)Cl]^{2+}$ Isomers[d] at 25.0 °C, μ = 1.0 ($NaClO_4$)

	λ, nm	pH[b]	$10^7[OH^-]$,[a] mol dm^{-3}	$10^3 k_{obsd}$, s^{-1}	$10^{-4} k_{calcd}$,[c] mol^{-1} dm^3 s^{-1}
anti-*p*	550	5.83 (M)	0.115	0.583	5.1
	340	6.92 (H)	1.41	7.52	5.3
	340	7.31 (H)	3.47	17.1	4.9
	340	7.93 (H)	14.5	79.7	5.5
	340	10.05 (G)	1910	9990	5.2
syn-*p*	550	5.85 (M)	0.12	0.051	0.43
	340	7.31 (H)	3.47	0.764	0.22
	340	7.87 (H)	12.6	2.41	0.19
	340	10.00 (G)	1700	322	0.19
s	550	5.90 (M)	0.135	0.056	0.41
	340	7.78 (T)	10.2	4.87	0.48
	340	8.19 (T)	26.3	13.1	0.50
	340	8.70 (T)	85.1	37.1	0.44
	340	8.70 (T)	85.1	35.7	0.42

[a] Calculated with pK_w = 13.77. [b] Buffers used: M = "MES"; H = HEPES; G = glycine; T = Tris. [c] k_{calcd} (mol^{-1} dm^3 s^{-1}) = $k_{obsd}/[OH^-]$. [d] $[Co] = (1.5 \times 10^{-3})-(8 \times 10^{-4})$ mol dm^{-3}.

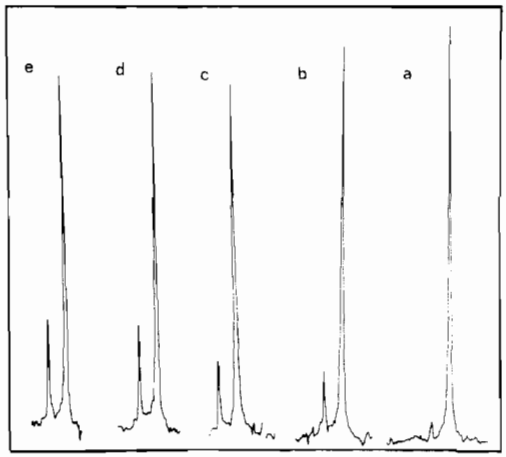

Figure 10. ^{13}C NMR spectra for isomerization of *anti-p*-$[Co(Me(tren))(NH_3)OH]^{2+}$ in 1 mol dm^{-3} NaOD (9.6% ^{13}C-enriched complex). From right to left t = 3, 12, 20, 30, and 40 min. The signal appearing at the lower field is that for the *s*-hydroxo isomer.

as shown by the data in Table X. The order of k_{OH} values anti-*p* $(5.2 \pm 0.2) \times 10^4$ mol^{-1} dm^3 s^{-1}, *s* $(0.45 \pm 0.02) \times 10^4$ mol^{-1} dm^3 s^{-1}, and syn-*p* $(0.19 \pm 0.02) \times 10^4$ mol^{-1} dm^3 s^{-1} at 25.0 °C and μ = 1.0 ($NaClO_4$) (the k_{obsd} data at low pH for the syn-*p* isomer need to be corrected for the normal aquation contribution of 3.0×10^{-5} s^{-1}) probably reflects the order of acidities of the NH proton responsible for the conjugate base part of the mechanism if the above explanation regarding steric crowding for loss of chloride holds here also. Certainly H exchange of some of the NH protons in the anti-*p* isomer is especially rapid ($k_{ex} > 10^7$ mol^{-1} dm^3 s^{-1}) although that on the *sec*-N center adjacent to chloride is not responsible (see above). These values of k_{OH} are to be compared with the value of 4×10^2 mol^{-1} dm^3 s^{-1} for the unsubstituted *p*-$[Co(tren)(NH_3)Cl]^{2+}$ ion;[9] steric acceleration in rate was also found for the loss of NH_3 from the analogous 3+ diammine ions.[3]

5. Isomerization in the $[Co(Me(tren))(NH_3)OH]^{2+}$ and $[Co(Me(tren))(NH_3)OH_2]^{3+}$ Ions. These data were necessary to adjust the observed products of base hydrolysis and induced aquation for the small amount of isomerization in the products during the reaction and/or measurement. Isomerization in the hydroxo ions was followed by ^{13}C NMR with use of the 30% ^{13}C-enriched material produced by base hydrolysis of the anti-*p*- and syn-*p*-chloro isomers. Typical data for the products from the anti-*p*-$[Co(Me(tren))(NH_3)Cl]^{2+}$ ion in 1.0 mol dm^{-3} NaOD are shown in Figure 10. At t = 0 base hydrolysis gives ca. 100% anti-*p* hydroxo product as shown by the signal at higher field, but this product slowly equilibrates to give some *s* isomer as shown by the appearance of the lower field singlet. This latter signal contains no (<5%) syn-*p* isomer as shown by acidification and ^1H NMR. In acidic solution the *s* isomer is clearly distinguished from the syn-*p* species in the proton spectrum. The rate for this equilibration process in 1.0 mol dm^{-3} NaOD, $(19 \pm 1) \times 10^{-4}$ s^{-1} at 19 °C, was also obtained in a similar experiment starting with the syn-*p*-chloro isomer. This would be expected if mutarotation to anti-*p* were rapid in the syn-*p*-hydroxo product under these conditions. The same rate was found in 0.1, 1.0, and 2.0 mol dm^{-3} NaOD. From the final product distribution, 27 ± 0.5% *s*- and 73 ± 0.5% *anti-p*-$[Co(Me(tren))(NH_3)OH]^{2+}$, the individual rates

$$\text{anti-}p\text{-OH} \underset{k_{31}}{\overset{k_{13}}{\rightleftharpoons}} s\text{-OH}$$

can be calculated; 6.6×10^{-4} s^{-1} (k_{31}) and 2.4×10^{-4} s^{-1} (k_{13}). Clearly the stability order anti-*p* > *s* > syn-*p* holds for the hydroxo ions.

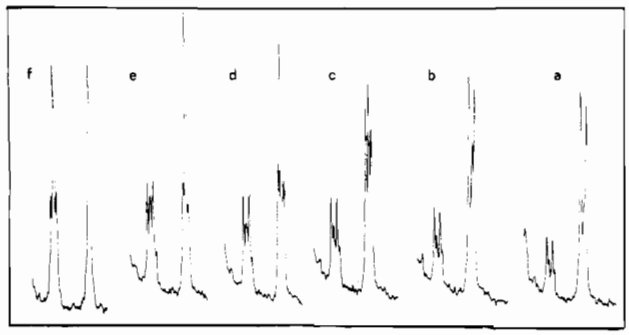

Figure 11. ^1H NMR spectra for isomerization of *s*-$[Co(Me(tren))(NH_3)OH_2]^{3+}$ (produced by Hg^{2+}-induced aquation of the *s*-chloro complex) in 0.1 mol dm^{-3} $DClO_4$. The disappearance of the *s*-aqua complex (2.20 ppm) accompanies the appearance of the anti-*p*-aqua complex (2.56 ppm). H exchange occurs in both ions as seen by the growth of the central singlets. From right to left t = 1, 4, 70, 130, and 195 min and 18 h. Only signals in the methyl group region are shown.

In a similar fashion isomerization in the syn-*p*- and *s*-aqua complexes was followed by ^1H and ^{13}C NMR, respectively, with use of the products generated by the Hg^{2+}-induced removal of chloride from the chloro isomers. That produced from the Hg^{2+}-induced reaction on the anti-*p* isomer (60% anti-*p*, 9% *s*, 31% syn-*p*) was too close to the final equilibrium distribution to provide useful data. Figure 11 shows representative ^1H NMR data during isomerization of the aqua products produced from *s*-$[Co(Me(tren))(NH_3)Cl]^{2+}$. The high-field doublet (2.20 ppm) for the *s*-aqua ion slowly decreases in intensity as that for the anti-*p* ion at lower field (2.56 ppm) grows. With use of the integrated intensity of the former a plot of log $(I_t - I_\infty)$ vs. time was linear with a rate constant of $(7 \pm 1) \times 10^{-5}$ s^{-1} (26 °C). H exchange is also apparent in both aqua ions as shown by the slow appearance of the central singlets, but it is clear that the *s* to anti-*p* change results from an isomerization (i.e., water-exchange) process rather than mutarotation (i.e., H exchange) since the latter ion is produced substantially without H exchange. H exchange in the anti-*p*-aqua isomer is somewhat slower than that in the *s* isomer (ca. 3×10^{-5} and ca. 1×10^{-3} s^{-1}, respectively).

Figure 12 gives representative ^{13}C data for the disappearance of the syn-*p*-aqua isomer produced by treatment of the corresponding chloro complex with Hg^{2+}. The t = 0 distribution of 85 ± 3% syn-*p*, 4 ± 2% anti-*p*, and 11 ± 1% *s* (from ^{13}C and ^1H data, see below) slowly changes to the equilibrium value of 6.5 ± 2% syn-*p*, 57 ± 2% anti-*p*, and 36.5 ± 2% *s*. The rate of appearance of the anti-*p* isomer is estimated at $(2.1 \pm 0.1) \times 10^{-4}$ s^{-1} (20 °C).

By considering the scheme

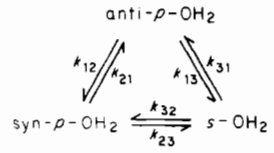

we have from the equilibrium distribution $k_{31}:k_{13}$ = 1.5 and $k_{21}:k_{12}$ = 8 and from the rate data the approximate equalities $k_{31} + k_{13} = 7 \times 10^{-5}$ s^{-1} and $k_{12} + k_{21} = 2.1 \times 10^{-4}$ s^{-1}. Thus $k_{13} \simeq 2.8 \times 10^{-5}$ s^{-1}, $k_{31} = 4.2 \times 10^{-5}$ s^{-1}, $k_{21} \simeq 1.9 \times 10^{-4}$ s^{-1}, and $k_{12} \simeq 2 \times 10^{-5}$ s^{-1}. Due to the complex nature of the equilibria involved these are only approximate rates. However, it is clear that the order of stabilities anti-*p* > *s* > syn-*p* for the aqua ions is the same as that found for the hydroxo and chloro complexes.

6. Stereochemistry and Mechanism of the Hg^{2+}-, Ag^+-, and NO^+-Induced Aquation Reactions. The products of the treatment of the three "red" chloro isomers with 1.0 mol dm^{-3}

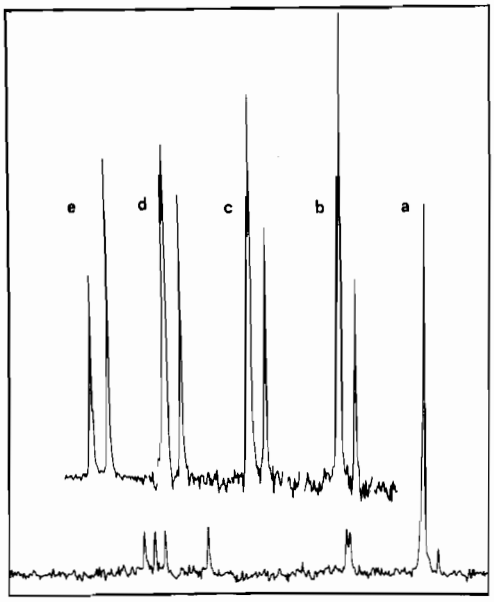

Figure 12. ^{13}C NMR spectra for isomerization in the *syn-p*-$[Co(Me(tren))(NH_3)OH_2]^{3+}$ ion (produced by Hg^{2+}-induced aquation of the *syn-p*-chloro complex) in 0.1 mol dm^{-3} $DClO_4$. The bottom trace gives the $t = 0$ spectrum (9.6% ^{13}C enriched), and the insets give the methyl region after 1.3, 1.7, 2.2, and 12 h (right to left). The disappearance of the *syn-p*-aqua isomer is accompanied by the appearance of the *anti-p*-aqua (1.23 ppm, higher field) and *s*-aqua isomers (0.18 ppm, lower field). The final distribution corresponds to 36.5 ■ 2% *s*, 6.5 ± 2% syn-*p*, and 57 ± 2% anti-*p* (see text) isomers.

Table XI. Products[a] of the Hg^{2+}-, Ag^+-, and NO^+-Induced Reactions of the *anti-p*-, *syn-p*-, and *s*-$[Co(Me(tren))(NH_3)X]^{2+}$ Isomers[b]

	X	reagent	% anti-*p*	% syn-*p*	% *s*
anti-*p*	Cl	Hg^{2+}	60	9	31
	Br	Hg^{2+}	60	4	36
	Cl	Ag^{2+}	59	4	37
	Br	Ag^+	55	5	40
	N_3	NO^+	50	7	43
syn-*p*	Cl	Hg^{2+}	4	85	11
	Br	Hg^{2+}	~2	90	8
	Cl	Ag^{2+}	12	64	24
	Br	Ag^+	10	70	20
	N_3	NO^+	12	62	26
s	Cl	Hg^{2+}	16	17	67
	Br	Hg^{2+}	24	4	72
	Cl	Ag^+	13	12	75
	Br	Ag^{2+}	18	12	70
	N_3	NO^+	28	2	70

[a] Extrapolated to zero time. [b] For the Hg^{2+}-induced reactions at least four separate experiments were done for X = Cl and duplicates for X = Br. For the Ag^+ and NO^+ experiments duplicate experiments were carried out.

Hg^{2+} in $DClO_4$ at pH 1 were determined by ^1H and ^{13}C NMR with use of the $^{13}CH_3$-enriched complexes. Figure 13 shows representative results, and it is clear the ^1H spectrum distinguishes the *s* from the anti-*p* + syn-*p* aqua complexes while the ^{13}C spectrum distinguishes the anti-*p* from *s* + syn-*p*. Several experiments were carried out on each isomer, and Table XI lists the product distributions at $t = 0$ (after allowance has been made for the small amount of isomerization during the reaction and/or measurement). Similar experiments were carried out on the bromo complexes.

Likewise, similar experiments were carried out in 0.1 mol dm^{-3} $DClO_4$ in the presence of excess $AgClO_4$ or with a twofold excess of $NaNO_2$. Table XI includes these results. The Ag^+-induced removal of chloride took ~30 min to complete, necessitating serious (~20% for the syn-*p* isomer) extrapolation of the data. The NO^+-induced reactions were complete within 2 min.

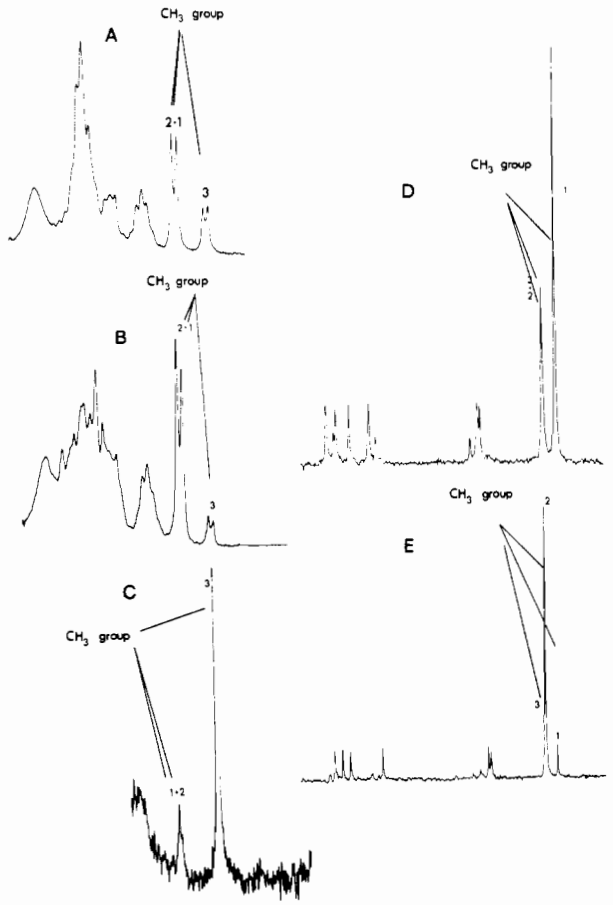

Figure 13. ^1H and ^{13}C NMR spectra of the products of the Hg^{2+}-induced aquation of the three "red" $[Co(Me(tren))(NH_3)Cl]^{2+}$ isomers, in 0.1 mol dm^{-3} $DClO_4$: (A) anti-*p* (^1H); (B) syn-*p* (^1H); (C) *s* (^1H); (D) anti-*p* (^{13}C, 9.6% ^{13}C enriched); (E) syn-*p* (^{13}C, 9.6% ^{13}C enriched). The methyl resonances are as follows: (1) anti-*p*-aqua; (2) syn-*p*-aqua; (3) *s*-aqua.

Two general conclusions can be made from these results: (1) substantial, but incomplete, stereochemical retention obtains for each reaction and (2) the product distributions show a leaving-group dependence.

The second result clearly holds when comparisons are made between the NO^+- and Hg^{2+}-induced reactions, and a real difference also occurs in the Hg^{2+} and Ag^+ reactions. Thus for the syn-*p* isomer 62% retention occurs with NO^+ and 85% with Hg^{2+}. A similar difference obtains in the Hg^{2+}, Ag^+ comparison. Also, some 17% syn-*p* product is produced from the *s* isomer with Hg^{2+}, 12% with Ag^+, and 2% with NO^+. The retention also seems larger the more bulky the leaving group when the reactions of the *s*- and syn-*p*-chloro and -bromo isomers with Hg^{2+} are compared. Also, substantially more (17%) of the syn-*p*-aqua product is formed from the *s*-chloro than from the *s*-bromo isomer.

These results clearly prohibit the formation of common intermediates, and for the NO^+ and Hg^{2+} reactions at least this seems in accord with the recent results for (+)-$[Co(en)_2BrX]^+$ (X = Br, N_3)[32] although this later result may be a little unusual.[32] Competition experiments (H_2O, NO_3^-) with the *t*-$[Co(tren)(NH_3)X]^{2+}$ species (X = Cl, N_3) also require the Hg^{2+} and NO^+ reactions to be different.[2] A note of caution must be added however in that the rate law dependence on the anionic component in solution has not been determined

(32) W. G. Jackson and A. M. Sargeson, *Inorg. Chem.*, **17**, 1348 (1978).

in these experiments and a difficulty may occur in this regard. Thus the reaction of NO^+ with $[Co(NH_3)_5N_3]^{2+}$ has been shown to have substantial Cl^-, NO_3^-, and ClO_4^- dependencies,[5,33] and a similar result has recently been shown for the Hg^{2+} reaction.[34] However, while altering the nature of the leaving group, these rate law variations do not preclude the subsequent formation of 5-coordinate species, and it is clear that in this regard a common intermediate is not involved. Also, the differences between X = Cl and X = Br remain.

The second result, that substantial retention of stereochemistry obtains for the same reaction between the different isomers, prohibits the formation of common intermediates between these species and gives a different insight into the mechanism. An examination of molecular models shows a close similarity between the isomers once the leaving group is disregarded, with only 30° movements of Co–N bonds in the equatorial plane being required to form the symmetrical trigonal bipyramid. Although the symmetrical form is unlikely to be that of lowest energy (in view of the methyl substituent), it serves to demonstrate their near equivalence. Also, incomplete retention of stereochemistry is an unusual result, with complete retention being normal (cf. $[Co(NH_3)_5X]^{2+}$ [35] and $[Co(en)_2(NH_3)X]^{2+}$ [36]); however, different products have been observed for (+)-$[Co(en)_2AX]^+$ (A = Cl, Br; X = Cl, Br, N_3).[32] The present result serves to demonstrate the flexibility of the ligand structure and the central metal atom toward incoming ligands, and energy differences for the different steric requirements of entry must be small. Even so the decided retention argues strongly that the solvent structure about the reactant ion is at least partly maintained, at least to the extent that it plays an important role in directing the entry of the incoming group. This allows two possible situations, first that the entering ligand takes some part in the process prior to the complete severance of the Co^{3+}–XHg^+ or Co^{3+}–N_3NO bond (i.e., an enforced I_a process) or that complete severance takes place before any attachment to the entering group occurs (I_d or S_N1 (lim)). The first process would predict an entering-group dependence in the rate law, but for water of course this is not observable. If the latter mechanism occurs, the 5-coordinate intermediate must be more reactive than the time necessary to rearrange groups within the encounter complex (i.e., the solvent cage). Its lifetime could well be governed by the loss of the entering nucleophile from the water structure, and it may survive only a few collisions within the encounter complex. Such requirements have only recently been clearly distinguished by Reenstra and Jencks.[37,38] A distinction between the two possibilities outlined is not possible from the present type of experiment, but it is clear that if a stepwise process were involved the lifetime of the 5-coordinate intermediate must be very short indeed (i.e., $<10^{-11}$ s). A distinction may be possible if the 5-coordinate species involves a spin change on the metal when very low concentrations or a spin-induced nuclear Overhauser effect may allow detection.

7. Base Hydrolysis Reaction. Base hydrolysis was carried out in 0.1, 1.0, and 2.0 mol dm^{-3} NaOD for the three chloro isomers and in 2.0 mol dm^{-3} NaOD for the bromo and diammine[3] complexes. The distributions were again determined by ^{13}C and ^1H NMR on the acidified solutions, and the results given in Table XII are extrapolated to $t = 0$ to allow for some small amount of isomerization in the hydroxo ions. Both the anti-*p*- and syn-*p*-chloro and-bromo complexes give exclusively the anti-*p*-hydroxo product, and the *s* isomer gives a substantial amount of retention. A similar result obtains for the *anti-p*- and *s*-$[Co(Me(tren))(NH_3)_2]^{3+}$ ions in 2.0 mol dm^{-3} NaOD. It is also clear that a different result obtains for X = Cl and X = NH_3 for both the anti-*p* and *s* complexes and that the results differ from the equilibrium distribution for the hydroxo ions of 73% anti-*p*, 27% *s*, and 0% syn-*p*.

Table XII. Products[a] of Base Hydrolysis of the *anti-p*- and *s*-$[Co(Me(tren))(NH_3)X]^{2+/3+}$ Isomers (X = Cl, Br, NH_3) and of *syn-p*-$[Co(Me(tren))(NH_3)X]^{2+}$ (X = Cl, Br)[c]

	X	[NaOD],[b] mol dm^{-3}	% anti-*p*	% syn-*p*	% *s*
anti-*p*	Cl	0.1	100	0	0
	Cl	1.0	100	0	0
	Cl	2.0	100	0	0
	Br	0.1	100	0	0
	NH_3	2.0	90	0	10
syn-*p*	Cl	0.1	100	0	0
	Cl	2.0	100	0	0
	Br	0.1	100	0	0
s	Cl	0.1	51	0	49
	Cl	1.0	58	0	42
	Cl	2.0	53	0	47
	Br	2.0	61	0	39
	NH_3	0.1	28	0	72
	NH_3	2.0	30	0	70

[a] Extrapolated to zero time (following acid addition). [b] Treatment for 30 s, followed by $DClO_4$ quench. [c] For X = Cl, NH_3 experiments were repeated; for X = Br, only one determination was made.

The same general conclusions can be made here as were made for the induced aquation reactions, i.e., that there is a leaving-group dependence in the products and that a common intermediate is not formed from the three isomers. This is especially clear for the *s* complexes, where different amounts of retention (~45% (Cl), 39% (Br), 70% (NH_3)) obtain, and this result differs from that obtained with the anti-*p* and syn-*p* isomers (0% *s*). No information is possible from the latter two reactants (except in the case of anti-*p*-NH_3) since ~100% anti-*p*-OH is formed in both cases. Mutarotation in the reactant does not occur prior to base hydrolysis as demonstrated by ^1H NMR experiments in DOAc buffers (although for the syn-*p* isomer H exchange on the *sec*-N center does occur prior to loss of chloride; see above), and it was shown that the mutarotation process occurred in the hydroxo product. Thus the anti-*p*–syn-*p* distribution is controlled by their concentrations at equilibrium (100%, 0%) and not by the immediate products of hydrolysis.

Differences in product distributions for different charged leaving groups have previously been noted in the base hydrolysis of (+)-$[Co(en)_2(NH_3)X]^{2+/3+}$ (X = Br^-, Me_2SO, TMP)[39] where a greater degree of retention was also found for the more highly charged ion. These differences are unlikely to result from the different sites for proton abstraction in the conjugate base part of the mechanism[40] since H-exchange studies on $[Co(NH_3)_6]^{3+}$ indicate that proton redistribution, or equilibration, between amine and amide sites occurs very rapidly and considerably faster than exchange between the amide site and the bulk solvent.[41] We prefer to support some retention of the solvent structure during loss of the leaving group and entry of water. Whether this occurs in a stepwise fashion or with some degree of concomitance is still open to question.

(33) D. A. Buckingham, C. R. Clark, and W. S. Webley, *Inorg. Chem.*, in press.
(34) W. L. Reynolds and E. R. Alton, *Inorg. Chem.*, **17**, 3355 (1978).
(35) D. A. Buckingham, I. I. Olsen, and A. M. Sargeson, *Aust. J. Chem.*, **20**, 597 (1967).
(36) D. A. Buckingham, I. I. Olsen, and A. M. Sargeson, *J. Am. Chem. Soc.*, **90**, 6654 (1968).
(37) W. W. Reenstra and W. P. Jencks, *J. Am. Chem. Soc.*, **101**, 5780 (1979).
(38) W. P. Jencks, *Acc. Chem. Res.*, **13**, 161 (1980).
(39) D. A. Buckingham, C. R. Clark, and T. W. Lewis, *Inorg. Chem.*, **18**, 1985 (1979).
(40) A. M. Sargeson, *Pure Appl. Chem.*, **33**, 527 (1973).
(41) E. Grunwald and D.-W. Fong, *J. Am. Chem. Soc.*, **94**, 7371 (1972).

Registry No. *anti-p*-(*R*,*S*)-[Co(Me(tren))(NH_3)Cl]($ZnCl_4$), 81521-71-3; $(+)_{505}$-*anti-p*-(*S*)-[Co(Me(tren))(NH_3)Cl]($ZnCl_4$), 81521-73-5; *s*-(*RS*)-[Co(Me(tren))(NH_3)Cl]($ZnCl_4$)·H_2O, 81505-45-5; *t*-[Co(Me(tren))(NH_3)Cl]Cl_2, 81497-06-5; $(-)_{505}$-*t*-[Co(Me(tren))(NH_3)Cl]((+)-$AsC_4H_2O_6)_2$, 81521-75-7; $(-)_{505}$-*t*-[Co(tren))(NH_3)Cl]Cl_2, 81521-76-8; *anti-p*-(*RS*)-[Co(Me(tren))(NH_3)Cl]($ClO_4)_2$, 81521-77-9; $(+)_{505}$-*anti-p*-(*S*)-[Co(Me(tren))(NH_3)Cl]((+)-$AsC_4H_2O_6)_2$, 81521-78-0; $(-)_{505}$-*anti-p*-(*R*)-[Co(Me(tren))(NH_3)Cl]($ZnCl_4$), 81521-80-4; *syn-p*-[Co(Me(tren))(NH_3)Cl]($ClO_4)_2$, 81521-81-5; *syn-p*-[Co(Me(tren))(NH_3)Cl]($ZnCl_4$), 81521-82-6; *syn-p*-[Co(Me(tren))(NH_3)Cl]Cl_2, 81521-64-4; *s*-[Co(Me(tren))(NH_3)Cl]($ClO_4)_2$, 81497-03-2; *anti-p*-[Co(Me(tren))(NH_3)Br]($ClO_4)_2$, 81570-13-0; *syn-p*-[Co(Me(tren))(NH_3)Br]($ClO_4)_2$, 81521-65-5; *s*-[Co(Me(tren))(NH_3)Br]($ClO_4)_2$, 81497-04-3; *anti-p*-[Co(Me(tren))(NH_3)N_3]($ClO_4)_2$, 81521-66-6; *s*-[Co(Me(tren))(NH_3)N_3]($ClO_4)_2$, 81497-05-4; *syn-p*-[Co(Me(tren))(NH_3)N_3]($CoO_4)_2$, 81521-67-7; *syn-p*-(*S*)-[Co(Me(tren))(NH_3)Cl]$^{2+}$, 81521-68-8; *syn-p*-(*R*)-[Co(Me(tren))(NH_3)Cl]$^{2+}$, 81521-69-9; *s*-(*S*)-[Co(Me(tren))(NH_3)Cl]$^{2+}$, 81521-70-2; *s*-(*R*)-[Co(Me(tren))(NH_3)Cl]$^{2+}$, 81521-59-7; *anti-p*-[Co(Me(tren))($NH_3)_2$]$^{3+}$, 69208-25-9; *s*-[Co(Me(tren))($NH_3)_2$]$^{3+}$, 69307-77-3; *t*-[Co(Me(tren))(NH_3)(OH_2)]$^{3+}$, 81497-00-9; *s*-[Co(Me(tren))(NH_3)(OH_2)]$^{3+}$, 81521-60-0; *anti-p*-[Co(Me(tren))(NH_3)(OH_2)]$^{3+}$, 81521-61-1; *syn-p*-[Co(Me(tren))(NH_3)(OH_2)]$^{3+}$, 81521-62-2; *anti-p*-[Co(Me(tren))(NH_3)(OH)]$^{2+}$, 81497-01-0; *s*-[Co(Me(tren))(NH_3)(OH)]$^{2+}$, 81521-63-3; Me(tren), 81497-21-4; Me(tren)·3HCl, 81497-22-5; [Co(Me(tren))($NO_2)_2$]Cl, 81497-02-1; [Co(Me(tren))Cl_2](ClO_4), 69991-09-9; tren, 4097-89-6; CH_3I, 74-88-4; (phenylsulfonyl)aziridine, 10302-15-5; 2,2′-diphthalimidodiethylamine, 63563-83-7; 2,2′-diphthalimido-2″-(benzenesulfamido)triethylamine, 81497-23-6; 2,2′-diphthalimido-2″-(*N*-methylbenzenesulfonamido)triethylamine, 81497-24-7; ethylenimine, 151-56-4; phthalic anhydride, 85-44-9; diethylenetriamine, 111-40-0.

Supplementary Material Available: Listings of crystal positional coordinates and thermal parameters (Table XIII), F_o and F_c (Table XIV), and hydrogen-bonding distances (Table XV) (24 pages). Ordering information is given on any current masthead page.

Contribution from the Department of Chemistry,
University of Windsor, Windsor, Ontario, Canada N9B 3P4

Direct Electrochemical Synthesis of Benzenethiolato Complexes of Tin(II), Tin(IV), and Lead(II). Molecular Structure of the 2,2′-Bipyridine Adduct of $Sn(SC_6H_5)_4$

J. LAWRENCE HENCHER, MASOOD KHAN, FAROUQ F. SAID, ROBERT SIELER, and DENNIS G. TUCK*

Received August 25, 1981

The electrochemical oxidation of tin into solutions of RSH (R = C_6H_5 $C_6H_4CH_3$) gives $Sn(SR)_2$. When 2,2′-bipyridine (bpy) or 1,10-phenanthroline is added to the solution phase, the product is the tin(IV) species $Sn(SR)_4L$. The electrochemical oxidation is shown to involve Sn(II) as the first product in each case. The crystal structure of $Sn(SC_6H_5)_4$bpy is monoclinic, with a = 13.150 (5) Å, b = 17.438 (6) Å, c = 14.215 (6) Å, β = 93.49 (3)°, V = 3254 (2) Å^3, Z = 4, and space group $P2_1/n$ (C_{2h}^5, No. 14). The molecule has a distorted octahedral SnS_4N_2 kernel, with bond distances of 2.449 (Sn–S) and 2.331 Å (Sn–N). With a lead anode, the product is $Pb(SC_6H_5)_2$; no lead(IV) species could be isolated.

Introduction

Compounds in which tin is bonded to a mercaptide ligand have been known for many years, and the preparative routes to $Sn(SR)_4$ compounds and the corresponding $R_nS(SR')_{4-n}$ species are well established.[1,2] Derivatives of tin(II) with such ligands are not so well-known, although some preparative and spectroscopic work has been reported.[3] Similarly, the chemistry of lead–thiolato compounds is well established.[4]

Applications of direct electrochemical synthesis in inorganic and organometallic chemistry have formed the subject of a number of recent papers from this laboratory. We have recently found that the electrochemical oxidation of a metal in the presence of thiols or disulfides is a convenient direct synthesis of neutral and anionic thiolato complexes of elements such as zinc, cadmium, mercury, gallium, indium, and thallium.[5,6] The present paper reports the extension of this work to tin and lead. Complexes with alkanethiolates were not obtained, but both tin(II), and lead(II) arenethiolates were easily prepared. Appropriate changes in the solution conditions gave rise to adducts of the tin(IV) thiolates with ligands such as 2,2′-bipyridine (bpy), although no such product could be obtained with lead. In the course of characterizing these materials, we carried out an X-ray structural analysis of $Sn(SC_6H_5)_4$·bpy, and the results of this study lead to a comparison with data for related compounds.

Experimental Section

General Data. Solvents were distilled and dried over molecular sieves. Tin metal was washed with concentrated aqueous hydrochloric acid and distilled water and dried immediately before use. Thiols were used as supplied as were 2,2′-bipyridine and 1,10-phenanthroline.

Metal analysis was by atomic absorption spectrophotometry. Microanalysis was performed by Guelph Chemical Laboratories Ltd.

Electrochemical Procedures. The electrochemical synthesis followed the methods described in earlier papers (e.g., ref 7), with a 100-mL tall-form beaker containing solutions of the composition shown in Table I. The cells were of the general form

$$Pt_{(-)}\,/\underset{\text{(acetone)}}{CH_3CN} + RSH\ \underset{\text{(phen)}}{(+\text{bpy})}\ /M_{(+)} \quad (M = Sn, Pb)$$

with the anode (~5 g) suspended into the solution phase on a platinum wire. The experiments were run in an atmosphere of dry nitrogen, with the solution magnetically stirred. Details of the isolation pro-

(1) Abel, E. W.; Armitage, D. A. *Adv. Organomet. Chem.* **1967**, *5*, 1.
(2) Schumann, H.; Schumann-Rudisch, I.; Schmidt, M. "Organotin Compounds"; Sawyer, A. K., Ed.; Marcel Dekker: New York, 1971; Vol. 2, p 297.
(3) Harrison, P. G.; Stobart, S. R. *Inorg. Chim. Acta* **1973**, *7*, 306 and references therein.
(4) Abel, E. W. "Comprehensive Inorganic Chemistry"; Trotman-Dickenson, A. F., Ed.; Pergamon Press: Oxford, 1973; Vol. 2, p 134.
(5) Hencher, J. L.; Khan, M.; Said, F. F.; Tuck, D. G. *Inorg. Nucl. Chem. Lett.* **1981**, *17*, 287.
(6) Said, F. F.; Tuck, D. G. *Inorg. Chim. Acta* **1982**, *59*, 1, and unpublished results.
(7) Habeeb, J. J.; Tuck, D. G. *Inorg. Synth.* **1979**, *19*, 257.

0020-1669/82/1321-2787$01.25/0